PHYSICAL REVIEW A VOLUME 22, NUMBER 2 AUGUST 1980

Double-quantum cross-polarization NMR in solids*

S. Vega, T. W. Shattuck, and A. Pines
Department of Chemistry and Materials and Molecular Research Division, Lawrence Berkeley Laboratory, University of California, Berkeley, California 94720
and Department of Isotope Research, The Weizmann Institute of Science, Rehovot, Israel
(Received 10 December 1979)

Double-quantum NMR is a useful way to obtain spectra of quadrupolar nuclei (^{2}D, ^{14}N, ...) in solids. This allows measurements of the chemical shifts for these nuclear spins. The theory of Hartmann-Hahn cross polarization between $I = 1/2$ and such $S = 1$ spins is discussed. Particular attention is drawn to the cross polarization of the double-quantum transition. The thermodynamics and the dynamics of the process are evoked in detail using a fictitious spin-1/2 formalism. The spin $S = 1$ Hamiltonian can always be factored into two commuting parts (independent thermodynamic reservoirs), one of which behaves as a fictitious spin 1/2 which is cross polarized with the $I = 1/2$ spins. Modified Hartmann-Hahn conditions emerge from the theory, and the dependence of cross-polarization times T_{IS} on rf intensity and frequency for spin locking and adiabatic demagnetization in the rotating-frame experiments are calculated. Measurements on the ^{1}H-^{2}D double resonance in dilute solid benzene-d_1 are reported, verifying the predictions and indicating that cross polarization provides a sensitive means of detecting the ^{2}D double-quantum transition. Values are reported for the thermodynamic parameters and cross-polarization times as a consequence. Three possible versions of double-resonance detection of double-quantum spectra are possible—direct detection of the cross-polarized double-quantum decay, indirect detection of the frequency spectrum following Hartmann and Hahn, and indirect detection of the free-induction decay following Mansfield and Grannell.

I. INTRODUCTION

Recently it was demonstrated that it is possible to obtain chemical shift spectra of deuterium nuclei in solids from novel NMR techniques.[1-3] In these experiments the coherence of the "forbidden" ($\Delta M = 2$) double-quantum transitions of these spins ($I = 1$) was excited and its time-dependent behavior was monitored.[4-8] The spectral lines of the double-quantum transitions, which are obtained by Fourier transformation of the measured time dependence of the double-quantum coherence, are not shifted by the quadrupole interaction. This is unlike the spectral lines of the allowed ($\Delta M = 1$) transitions, which are split (and in powders therefore broadenend) due to this interaction. The small deuterium shifts, due to the chemical shielding in single crystals and powder samples, were obtained for the first time and compared with proton chemical shift data.[2,3] This technique makes it attractive to replace hydrogen atoms in solids partially by deuterium and to perform high-resolution NMR spectroscopy on the double-quantum transitions of the deuterium spins.[3,9] The spectral linewidths, due to dipole-dipole interactions between deuterium nuclei, can be made very narrow by sufficient dilution of the deuterium spins together with proton spin decoupling.

This rather simple approach forms a complementary method to the multiple-pulse techniques for the observation of high-resolution proton NMR in solids.[10] However, because of the very low abundance of the deuterium atoms in the solid, the measured signal intensities are very small and we would like to be able to apply cross-polarization techniques for signal enhancement.[11-15] In these experiments nuclear polarization is transferred between the abundant spin system and the rare nuclei in the sample. The polarization of the transitions of the rare spins can result in an enhancement of their NMR signal intensities. Alternatively, the free-induction decay of the S spins is monitored by observing the I spins using cross polarization. These methods are well understood and widely used for abundant spins (protons) and rare spins (like ^{13}C, ^{15}N, and ^{29}Si) where both spin systems have a spin value $I = \frac{1}{2}$. In our case it would be most attractive to cross polarize or detect the double-quantum coherence of the deuterium spins with $S = 1$ directly from the abundant protons. This would provide high-sensitivity double-quantum spectra directly. In this paper we discuss such NMR cross-polarization experiments between abundant nuclei with spin $I = \frac{1}{2}$ and rare nuclei with $S = 1$. We show experimentally and theoretically that it is indeed possible to polarize the double-quantum transition of deuterium from protons in a solid.

In Sec. II we review briefly the spin thermodynamics of cross-polarization experiments for two spin $I = \frac{1}{2}$ systems (e.g., ^{13}C–^{1}H), in order to form a basis for the new material in this paper. In Sec. III the theory of spin thermodynamics is extended to a spin $S = 1$, $I = \frac{1}{2}$ system. The fictitious spin-$\frac{1}{2}$ operators[1,16-18] used to describe single- and double-quantum coherences in the S-spin system

compactly, are introduced and used for the description of the thermodynamics of this spin system. The Hartmann-Hahn conditions for different cross-polarization experiments are derived. In Sec. IV the spin dynamics of the cross-polarization process is discussed. The theory of spin dynamics for spin $S=\frac{1}{2}$, $I=\frac{1}{2}$ systems[13,14,19] is extended to systems with $I=\frac{1}{2}$ and $S=1$. The relaxation phenomena during cross polarization of the single- and double-quantum transitions of the S-spin systems are described. In Sec. V experimental results are presented. These results are compared with the theoretical derivations in Secs. III and IV. The modified Hartmann-Hahn conditions for the single- and double-quantum double-resonance experiments are verified. The cross-polarization time in deuterated benzene in the solid state is measured and the ratio of the heat capacities of the I spins and the S spins in the solid is obtained from the experiments and compared with the theoretical value.

II. SPIN THERMODYNAMICS WITH $I=\frac{1}{2}$ AND $S=\frac{1}{2}$

In this section we review briefly the spin thermodynamics of the cross-polarization process between high-abundance spins $I=\frac{1}{2}$ and low-abundance spins $S=\frac{1}{2}$ in the solid.[13] The presentation of the theory of cross polarization in this section serves as a reminder of notation and equations required for the remainder of this paper. The Hamiltonian in the laboratory frame of the spin system under consideration, in an external magnetic field H_0 and with applied rf irradiation fields at the Larmor frequencies, can be represented by

$$H=-\omega_{0I}I_z-\omega_{0S}S_z-2\omega_{1I}I_x\cos\omega_{0I}t \\ -2\omega_{1S}S_x\cos\omega_{0S}t+H_{II}+H_{IS}\,, \tag{2.1}$$

with

$$S_p=\sum_{s=1}^{N_S}S_{ps}\,, \\ I_p=\sum_{i=1}^{N_I}I_{pi}\,,\quad p=x,y,z\,.$$

$\omega_{0I}=\gamma_I H_0$ and $\omega_{0S}=\gamma_S H_0$ are the Larmor frequencies of the I and S spins, respectively. γ_I and γ_S are the magnetogyric ratios of the I and S spins and $2\omega_{1I}$ and $2\omega_{1S}$ are the rf irradiation field intensities in frequency units.

$$H_{IS}=2\sum_{is}b_{is}I_{zi}S_{zs}\,, \\ b_{is}=-2\gamma_I\gamma_S\hbar r_{is}^{-3}P_2(\cos\theta_{is}) \tag{2.2}$$

and

$$H_{II}=\sum_{ij}a_{ij}(I_iI_j-3I_{zi}I_{zj})\,, \\ a_{ij}=\gamma_I^2\hbar r_{ij}^{-3}P_2(\cos\theta_{ij}) \tag{2.3}$$

are the secular parts of the magnetic dipole-dipole interactions with respect to the Zeeman interaction between the high-abundant I spins and the secular part of the dipole-dipole interaction between the I spins and the low-abundant S spins, respectively. The interaction between the S spins themselves is ignored because of their low abundance. The total spin system can be described by the spin density matrix ρ and in thermal equilibrium

$$\rho_{eq}=Z^{-1}\exp[-\beta_L(-\omega_{0I}I_z-\omega_{0S}S_z)]\,, \tag{2.4}$$

where we use the high-temperature approximation

$$Z=\mathrm{Tr}\{\exp[-\beta_L(-\omega_{0I}I_z-\omega_{0S}S_z)]\}\simeq\mathrm{Tr}(1)\,,$$

and where $\beta_L=1/kT_L$, with T_L the laboratory temperature.

In the rotating frame defined by the transformation operator

$$U_0=\exp[-it(\omega_{0I}I_z+\omega_{0S}S_z)]\,, \tag{2.5}$$

the density matrix becomes

$$\rho^*=U_0^{-1}\rho U_0 \tag{2.6}$$

and the Hamiltonian

$$H^*=-\omega_{1I}I_x-\omega_{1S}S_x+H_{II}+H_{IS} \\ =H_I^*+H_S^*+H_{IS} \tag{2.7}$$

with

$$H_I^*=-\omega_{1I}I_x+H_{II}\,, \\ H_S^*=-\omega_{1S}S_x\,. \tag{2.8}$$

The $*$ signs for the notation of operators in the rotating frame are dropped from now on, because all following equations and discussions apply to this frame.

With the spin temperature hypothesis the general form of the density matrix in the rotating frame is

$$\rho=Z^{-1}(1-\beta_I H_I-\beta_S H_S)\,, \tag{2.9}$$

where β_I and β_S are the spin temperature coefficients of the I-spin system and the S-spin system, respectively. According to Hartmann and Hahn, for an initial condition $\beta_I\neq\beta_S$ the two spin temperature coefficients will evolve to a common value β_f, due to the influence of H_{IS} on H_I and H_S. The rate of equilibration is strongly dependent on the rf irradiation field intensities. With the proper experimental conditions, this cross-polarization process can be used to enhance the NMR signals of the S spins. The intensities of these signals are

proportional to β_S and we therefore wish to increase this coefficient as much as possible by cooling the S-spin system.

A schematic representation of the cross-polarization process is given in Fig. 1. The enhancement of the S-spectral line intensities is performed by cooling the I spins first $\beta_I \gg \beta_L$, and then cross polarizing the two spin systems in order to increase β_S. Two types of experiments for the preparation of the I spin and the cross-polarization process are discussed here. In the first experiment the I spins are cooled by spin locking (SL) and during the cross-polarization period the Hartmann-Hahn condition

$$\omega_{1I} = \omega_{1S} \tag{2.10}$$

is fulfulled. The cooling of the I spins in the second experiment is performed by adiabatic demagnetization in the rotating frame (ADRF). In this case the cross-polarization process occurs with no applied rf irradiation field on the I spins. A schematic representation of these two experiments is given in Fig. 2. In both cases after the preparation of the I spins we have (using $\|\ \|$ to denote magnitude)

$$\|\beta_I H_I\| \gg \|\beta_S H_S\|$$

and the density matrix can be written as

$$\rho_{\text{initial}} = Z^{-1}(1 - \beta_I H_I)\,, \tag{2.11}$$

where we neglected the H_S term. After cross polarization the density matrix becomes

$$\rho_{\text{final}} = Z^{-1}[1 - \beta_f(H_I + H_S)]\,. \tag{2.12}$$

During the evolution period of ρ, energy is conserved and the initial energy E_{initial} of the total spin system is equal to the final energy E_{final}:

$$E_{\text{initial}} = E_{\text{final}}\,, \tag{2.13}$$

with

$$\begin{aligned} E_{\text{initial}} &= \mathrm{Tr}(\rho_{\text{initial}} H) = -Z^{-1}\beta_I \mathrm{Tr}(H_I^2)\,, \\ E_{\text{final}} &= \mathrm{Tr}(\rho_{\text{final}} H) \\ &= -Z^{-1}\beta_f[\mathrm{Tr}(H_I^2) + \mathrm{Tr}(H_S^2)]\,. \end{aligned} \tag{2.14}$$

In order to obtain explicit expressions for β_f from Eq. (2.13) we must distinguish between the SL experiment and the ADRF experiment. We therefore evaluate β_f and the enhancement of the S-spin intensities for the two techniques separately.

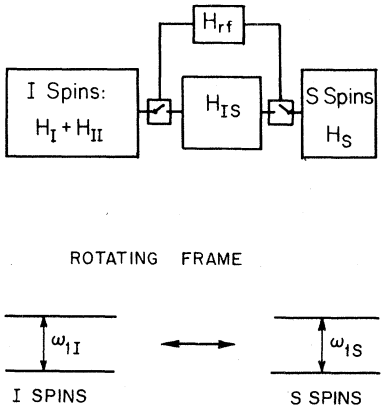

FIG. 1. Schematic representation of the cross-polarization process between two spin systems with spin values $I = S = \frac{1}{2}$. The spin systems have Hamiltonians $H_I + H_{II}$ and H_S, respectively. The two systems are connected by the magnetic dipolar interaction H_{IS}. This interaction causes an energy flow from the S spins to the I spins, if the applied rf irradiation field intensities ω_{II} and ω_{IS} have the right values ($H_{rf} = -\omega_{II} I_x - \omega_{IS} S_x$). In a spin-lock experiment these intensities must be taken according to the Hartmann-Hahn condition in Eq. (2.10) $\omega_{IS} = \omega_{II}$.

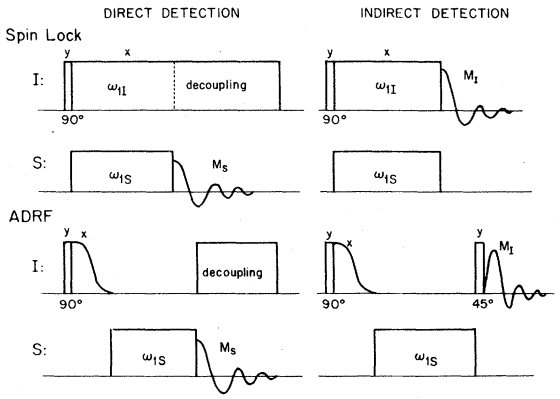

FIG. 2. Representation of four cross-polarization experiments on a spin system, consisting of high-abundant I spins and rare S spins. The two experiments at the top of the figure are spin-lock experiments. Here the I spins are prepared by a 90° pulse followed by a 90° phase shift of the rf irradaiation field. After this preparation the cross-polarization process takes place during the application of an additional rf field on the S spins. The intensity of this rf field must be chosen according to the Hartmann-Hahn condition. At the end of the cross polarization we can detect the increase of the S signal intensity directly (left) or monitor the polarization of the S spins indirectly by the detection of the decrease of the I signal intensity (right). At the bottom of the figure two ADRF experiments are represented. In these cases after the preparation of the I spins as in the spin-lock case, the rf irradiation field is decreased to zero. The cross polarization occurs again by the application of an rf field on the S spins. The direct detection of the S signal after the cross-polarization period is the same as for the spin-lock case. For the indirect detection we must apply an additional 45° pulse on the I spins in order to recover the I signal.

A. Spin locking experiment

In the spin-lock experiment the I spins are cooled by a 90° rf pulse followed by an immediate 90° phase change of the irradiation field in order to lock the I spins to this field. After this preparation we apply simultaneously an rf irradiation field on the I spins and the S spins according to the Hartmann-Hahn condition (2.10). The Hamiltonian in Eq. (2.7) with $\|\omega_{1I}I_x\| \gg \|H_{II}\|$ becomes

$$H = H_I + H_S = -\omega_{1I}I_x - \omega_{1S}S_x , \tag{2.15}$$

where we neglect H_{II} and H_{IS}

and

$$\rho_{\text{initial}} = e^{-i(\pi/2)I_y}\rho_{\text{eq}}e^{i(\pi/2)I_y} = Z^{-1}(1 - \beta_L\omega_{0I}I_x - \beta_L\omega_{0S}S_x) . \tag{2.16}$$

For convenience we transform the spin system by the unitary operator

$$U_{\text{SL}} = \exp[-i\tfrac{1}{2}\pi(I_y + S_y)] ,$$

in order to obtain the Hamiltonian in terms of operators in the z direction

$$H^T = U_{\text{SL}}^{-1} H U_{\text{SL}} = H_I^T + H_S^T = -\omega_{1I}I_z - \omega_{1S}S_z . \tag{2.17}$$

The initial density matrix is now written according to Eqs. (2.11) and (2.16) as

$$\rho_{\text{initial}}^T = U_{\text{SL}}^{-1}\rho_{\text{initial}}U_{\text{SL}} = Z^{-1}(1 - \beta_I H_I^T) , \tag{2.18}$$

with

$$\beta_I = \beta_L\omega_{0I}/\omega_{1I} , \tag{2.19}$$

which gives indeed $\beta_I \gg \beta_L$. After this preparation the I- and S-spin systems will evolve to a state given by

$$\rho_{\text{final}}^T = Z^{-1}[1 - \beta_f(H_I^T + H_S^T)] . \tag{2.20}$$

With Eqs. (2.13) and (2.14) it is now possible to calculate β_f with

$$\begin{aligned} E_{\text{initial}} &= Z^{-1}\beta_I\omega_{1I}^2\,\text{Tr}(I_z^2) = \beta_I C_I , \\ E_{\text{final}} &= Z^{-1}\beta_f[\text{Tr}(I_z^2) + \text{Tr}(S_z^2)] \\ &= \beta_f(C_I + C_S) , \end{aligned} \tag{2.21}$$

and

$$\beta_f = \frac{\beta_I C_I}{C_I + C_S} = \beta_I\left(1 + \frac{C_S}{C_I}\right)^{-1} . \tag{2.22}$$

The heat capacities C_I and C_S of the I and S spins, respectively, introduced in Eq. (2.21) are defined as

$$\begin{aligned} C_I &= \delta E/\delta\beta_I = -Z^{-1}\,\text{Tr}(H_I^T)^2 = Z^{-1}\omega_{1I}^2\,\text{Tr}(I_z^2) , \\ C_S &= \delta E/\delta\beta_S = -Z^{-1}\,\text{Tr}(H_S^T)^2 = Z^{-1}\omega_{1S}^2\,\text{Tr}(S_z^2) , \end{aligned} \tag{2.23, 2.24}$$

and with

$$Z^{-1} = (2I+1)^{N_I}(2S+1)^{N_S} \tag{2.25}$$

and

$$\begin{aligned} \text{Tr}(I_z^2) &= \text{Tr}\left(\sum_i I_{zi}^2\right) \\ &= \tfrac{1}{2}(2S+1)^{N_S}(2I+1)^{N_I-1} , \end{aligned} \tag{2.26}$$

$$\begin{aligned} \text{Tr}(S_z^2) &= \text{Tr}\left(\sum_S S_{zi}^2\right) \\ &= \tfrac{1}{2}(2I+1)^{N_I}(2S+1)^{N_S-1} , \end{aligned} \tag{2.27}$$

they become

$$C_I = \frac{1}{2}\frac{N_I}{2I+1}\omega_{1I}^2 = \tfrac{1}{4}N_I\omega_{1I}^2 \tag{2.28}$$

and

$$C_S = \frac{1}{2}\frac{N_S}{2S+1}\omega_{1S}^2 = \tfrac{1}{4}N_S\omega_{1S}^2 . \tag{2.29}$$

Realizing that $N_S \ll N_I$ and $\omega_{1S} \simeq \omega_{1I}$, the ratio ϵ between the heat capacities is very small

$$\epsilon = \frac{C_S}{C_I} = \frac{N_S}{N_I}\frac{\omega_{1S}^2}{\omega_{1I}^2} , \tag{2.30}$$

and to a good approximation we can write

$$\begin{aligned} \beta_f &= \beta_I(1+\epsilon)^{-1} \simeq \beta_I(1-\epsilon) \\ &= \beta_L(\omega_{0I}/\omega_{1I})(1-\epsilon) . \end{aligned} \tag{2.31}$$

B. ADRF experiment

The cooling of the I spins in the case of an adiabatic demagnetization in a rotating frame (ADRF) experiment is performed by first spin locking these spins to an rf field and then reducing this field to zero adabatically. The spins are then locked to their local fields due to their neighboring I spins. The initial condition of the spin system is here given by

$$\rho_{\text{initial}} = Z^{-1}(1 - \beta_I H_{II}) , \tag{2.32}$$

with

$$\beta_I = \beta_L\omega_{0I}/\omega_I , \tag{2.33}$$

where ω_I represents the local field intensity defined by

$$\omega_I^2 = \frac{\text{Tr}(H_{II}^2)}{\text{Tr}(I_x^2)} . \tag{2.34}$$

After the preparation of the I spins an rf field is applied to the S spins and the cross-polarization process will start. During the cross polarization we have

$$H = H_I + H_S = H_{II} - \omega_{1x}S_x \tag{2.35}$$

and in order to represent H in terms of S_z we again perform a transformation of the spin sys-

tem, but now defined by the operator

$$U_{\mathrm{ADRF}} = \exp(-i\tfrac{1}{2}\pi S_y) . \tag{2.36}$$

The Hamiltonian becomes

$$H^T = U^{-1}_{\mathrm{ADRF}} H U_{\mathrm{ADRF}} = H^T_{II} - \omega_{1S} S_z \tag{2.37}$$

and the final density matrix

$$\rho^T_{\mathrm{final}} = U^{-1}_{\mathrm{ADRF}} \rho_{\mathrm{final}} U_{\mathrm{ADRF}} = Z^{-1}[1 - \beta_f (H_{II} - \omega_{1S} S_z)] . \tag{2.38}$$

Energy conservation leads to a similar result as in Eq. (2.22) for β_f

$$\beta_f = \frac{\beta_I C_I}{C_I + C_S} , \tag{2.39}$$

with C_S as in Eq. (2.24) and

$$C_I = Z^{-1} \mathrm{Tr}(H^2_{II}) . \tag{2.40}$$

Here again because of $C_I \gg C_S$ we have

$$\beta_f = \beta_I (1 - \epsilon) .$$

C. Signal intensities

The results for β_f from the SL and the ADRF experiments can now be used to evaluate the increase in intensity of the S-spin signals after cross polarization. This signal intensity M_S must be compared with the S-signal intensity M°_S after a single 90° pulse on the S spins. The signal intensity M_S is proportional to β_f and can be represented by

$$M_S = \mathrm{Tr}(\rho^T_{\mathrm{final}} S_z) = Z^{-1} \omega_{1S} \beta_f \mathrm{Tr}(S^2_z) = \tfrac{1}{4} \beta_f N_S \omega_{1S} . \tag{2.41}$$

The signal intensity M°_S is easily calculated and equals

$$M^\circ_S = \mathrm{Tr}(\rho_{\mathrm{eq}} S_z) = Z^{-1} \omega_{0S} \beta_L \mathrm{Tr}(S^2_z) = \tfrac{1}{4} \beta_L N_S \omega_{0S} \tag{2.42}$$

and the ratio between these two signals becomes

$$\frac{M_S}{M^\circ_S} = \frac{\omega_{1S} \beta_f}{\omega_{0S} \beta_L} . \tag{2.43}$$

For the SL case and using Eq. (2.31) this ratio becomes

$$\frac{M_S}{M^\circ_S} = \frac{\omega_{0I}}{\omega_{0S}} \frac{\omega_{1S}}{\omega_{1I}} (1 - \epsilon) = \frac{\gamma_I}{\gamma_S} (1 - \epsilon) , \tag{2.44}$$

where we used the Hartmann-Hahn condition in Eq. (2.10). For the ADRF case we obtain the same result if we assume that

$$\omega_I = \omega_{1S} . \tag{2.45}$$

From (2.44) we see that for an SL or an ADRF experiment the enhancement of the S-signal intensity is γ_I/γ_S, which equals 4.2 for I spins ^{1}H and S spins ^{13}C.

In addition to the direct detection of the NMR signals of the S spins it is also possible to monitor the cross-polarization process by an indirect detection method.[12] In that case we monitor the decrease in the signal intensities of the I spins due to cross polarization. This can be done as a function of time by repolarizing after evolution of the S spins to monitor the high-resolution S free-induction decrease (see Fig. 15 of Ref. 13). In the SL experiment this signal intensity just after spin locking equals

$$M^\circ_I = \mathrm{Tr}(\rho^T_{\mathrm{initial}} I_z) = Z^{-1} \omega_{1I} \beta_I \mathrm{Tr}(I^2_z) = \tfrac{1}{4} N_I \omega_{1I} \beta_I \tag{2.46}$$

and after cross polarization

$$M_I = \mathrm{Tr}(\rho^T_{\mathrm{final}} I_z) = Z^{-1} \omega_{1I} \beta_f \mathrm{Tr}(I^2_z) = \tfrac{1}{4} N_I \omega_{1I} \beta_f . \tag{2.47}$$

The relative decrease in the I signal intensity is therefore [using β_f from (2.22)]

$$\frac{M^\circ_I - M_I}{M^\circ_I} = \frac{\beta_I - \beta_f}{\beta_I} = \epsilon . \tag{2.48}$$

This is modified to $\epsilon[2 - S(t)]$, where $S(t)$ is the S free-induction decay, for the experiment of Ref. 12.

The small change in M_I due to the cross-polarization process gives a measure for the ratio of the heat capacities of the S spins and the I spins. For ADRF a similar result is obtained for the relative ratio in Eq. (2.48).

III. SPIN THERMODYNAMICS WITH $I = \frac{1}{2}$, $S = 1$

A. Introduction

We describe here the thermodynamics of cross polarization for the case of abundant spins $I = \frac{1}{2}$ and rare spins $S = 1$. Because the S-spin system is a three-nuclear-spin-energy-level system, the theory of cross polarization for this system is somewhat richer than the $I = \frac{1}{2}$, $S = \frac{1}{2}$ case. However, we realize that under appropriate conditions in an NMR experiment the cross-polarization process occurs only between the I spins and one of the transitions of the S spins. Both the two allowed transitions ($\Delta M = 1$) and the forbidden double-quantum transition ($\Delta M = 2$) can cross polarize separately with the I spins, depending on the experimental conditions. The cross-polarizing transition of the S spins can be treated as a fictitious spin-$\frac{1}{2}$ transition and the part of the S-spin system corresponding to this transition, together with the I spins, forms a spin system similar to the one discussed in Sec. II. Therefore we can use the

formalism of Sec. II to describe the cross-polarization process for the $I=\frac{1}{2}$, $S=1$ case, and this simplifies the theoretical derivations of the spin thermodynamics.

In this section we discuss the spin thermodynamics of cross polarization for each individual transition of the S spins separately. For each case the corresponding Hartmann-Hahn condition is derived, spin temperatures are calculated, and the signal intensities from direct and indirect detection measurements are obtained. To simplify the actual calculations we first introduce the fictitious spin-$\frac{1}{2}$ operator formalism for the S-spin system. Then the general theory of cross polarization is given and finally explicit expressions are derived.

B. Spin system with $S = 1$

Fictitious spin-$\frac{1}{2}$ operator formalism

It was shown that for the description of NMR experiments on multilevel spin systems, it is convenient to express the Hamiltonian and the spin density matrix in terms of fictitious spin-$\frac{1}{2}$ operators.[1,17,18] For spins $S=1$ the matrix elements of these operators are defined in the basis set

$$|1\rangle = |+1\rangle, \quad |2\rangle = |0\rangle, \quad |3\rangle = |-1\rangle, \tag{3.1}$$

where $|+1\rangle$, $|0\rangle$, and $|-1\rangle$ are the eigenstates of S_z of the S spins. The operators are defined by their nonzero matrix elements using the notation

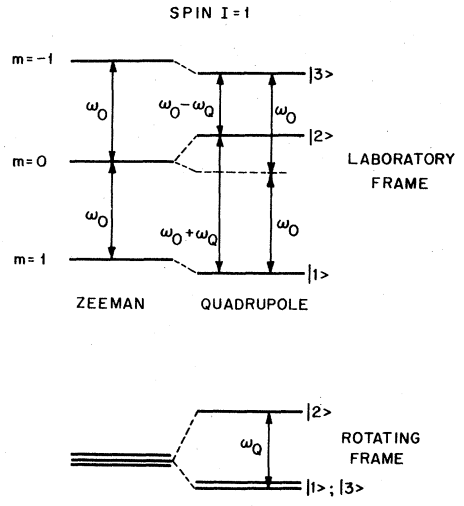

FIG. 3. Energy level diagrams of a spin $S=1$ in a solid in an external magnetic field. The Zeeman and quadrupolar frequency shifts are shown in the laboratory frame and in the rotating frame. The eigenstates of S_z are $|1\rangle$, $|2\rangle$, and $|3\rangle$ with $m=1$, 0, and -1, respectively.

of Vega[17]:

$$\begin{aligned}
&\langle i|S_x^{i-j}|j\rangle = \langle j|S_x^{i-j}|i\rangle = \tfrac{1}{2}, \\
&\langle i|S_y^{i-j}|j\rangle = -\langle j|S_y^{i-j}|i\rangle = \tfrac{1}{2}i, \\
&\langle i|S_z^{i-j}|i\rangle = -\langle j|S_z^{i-j}|j\rangle = \tfrac{1}{2},
\end{aligned} \tag{3.2}$$

and we see immediately that the operators S_p^{1-2} and S_p^{2-3} with $p=x,y,z$ form the single-quantum operators, while S_p^{1-3} are the double-quantum operators. With these definitions we obtain

$$\begin{aligned}
S_x &= \sqrt{2}(S_x^{1-2}+S_x^{2-3}), \\
S_y &= \sqrt{2}(S_y^{1-2}+S_y^{2-3}), \\
S_z &= 2S_z^{1-3} = 2(S_z^{1-2}+S_z^{2-3}),
\end{aligned} \tag{3.3}$$

and with $[S_p^{i-j}, S_q^{i-j}] = iS_r^{i-j}$ where $p,q,r=x,y,z$ or cyclic permutations we have

$$U_p^{i-j}(-\theta)S_q^{i-j}U_p^{i-j}(\theta) = S_q^{i-j}\cos\theta + S_r^{i-j}\sin\theta,$$

where

$$U_p^{i-j}(\theta) = \exp(i\theta S_p^{i-j}).$$

Additional commutation relations between the S_p^{i-j} operators are given elsewhere.[17,18]

Hamiltonian

The Hamiltonian of the S spins in a solid in an external magnetic field $H_0=\omega_{0S}/\gamma_S$ and with an rf irradiation field at frequency ω and intensity ω_{1S}, becomes in the rotating frame

$$H = -\Delta\omega S_z + \tfrac{1}{3}\omega_Q[S_z^2 - S(S+1)] - \omega_{1S}S_x, \tag{3.4}$$

with the quadrupole frequency

$$\omega_Q = \tfrac{1}{4}e^2qQ[\tfrac{1}{2}(3\cos^2\theta - 1) + \eta\sin^2\theta\cos 2\phi]$$

and the off-resonance frequency

$$\Delta\omega = \omega_0 - \omega.$$

In terms of the fictitious spin-$\frac{1}{2}$ operators, H becomes

$$\begin{aligned}
H = &-2\Delta\omega S_z^{1-3} + \tfrac{2}{3}\omega_Q(S_z^{1-2} - S_z^{2-3}) \\
&- \sqrt{2}\omega_{1S}(S_x^{1-2} + S_x^{2-3})
\end{aligned} \tag{3.5}$$

and the general form of the density matrix is

$$\rho = a_0 1 + \sum_{i<j}\sum_{p=x,y,z} a_p^{i-j}S_p^{i-j}, \tag{3.6}$$

with

$$a_p^{i-j} = \mathrm{Tr}(\rho S_p^{i-j}).$$

A schematic representation of ρ is given in Fig. 4. In this representation we assign to each transition a coordinate system with axes x^{i-j}, y^{i-j}, and z^{i-j} and we define ρ by one vector in each of these systems. The three vectors are not totally independent because the S_z^{i-j} operators are not indepen-

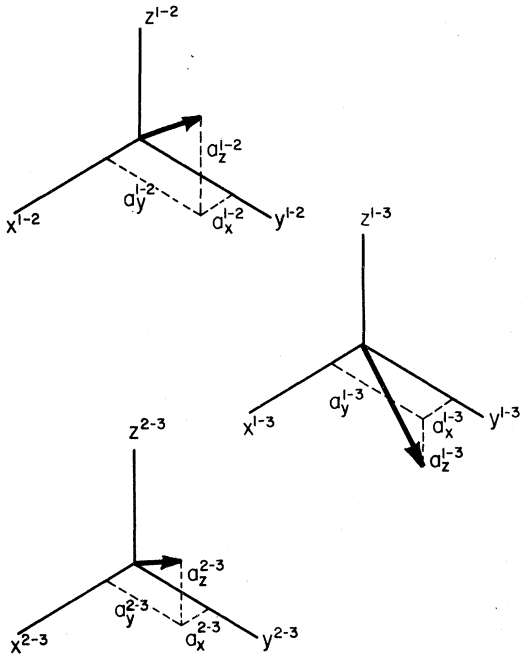

FIG. 4. A vector representation of the density matrix ρ of a spin $S=1$. In terms of the fictitious spin-$\frac{1}{2}$ angular momentum operators we can write $\rho = a_0\, 1 + \sum_{i=1}^{3} \times \sum_{p=x,y,z} a_p^{i-j} I_p^{i-j}$. For each possible combination i-j we define a coordinate system which contains a vector $(a_x^{i-j}, a_y^{i-j}, a_z^{i-j})$. In our case three systems with three vectors describe the density matrix ρ. Notice the dependence of the components of these vectors $a_z^{1-2} + a_z^{2-3} - a_z^{1-3} = 0$.

dent:

$$S_z^{i-j} = S_z^{i-k} + S_z^{k-j}. \tag{3.7}$$

The behavior in time of ρ can be represented by the motion of these vectors due to the effective field each of them feels.

Irradiation near allowed transition ($\Delta\omega \sim \omega_Q$)

For an rf irradiation field at a frequency close to one of the satellites of the S spectrum $\Delta\omega = \omega_Q + \delta\omega$ the Hamiltonian becomes

$$H_s = -2(\omega_Q + \delta\omega)(S_z^{1-2} + S_z^{2-3}) + \tfrac{2}{3}\omega_Q(S_z^{1-2} - S_z^{2-3}) - \sqrt{2}\omega_{1S}(S_x^{1-2} + S_x^{2-3})$$

and with Eq. (3.7) and $\omega_{1S},\ \delta\omega \ll \omega_Q$

$$H_S \simeq -\delta\omega S_z^{1-2} - \sqrt{2}\omega_{1S} S_x^{1-2} - (\tfrac{4}{3}\omega_Q + \delta\omega)(S_z^{1-3} + S_z^{2-3}). \tag{3.8}$$

In order to change the irradiation term in H_S to a Zeeman-like term, we transform H_S with the unitary operator

$$U_y^{1-2}(\tfrac{1}{2}\pi) = \exp(i\tfrac{1}{2}\pi S_y^{1-2})$$

and we get

$$H_S^T = U_y^{1-2}(-\tfrac{1}{2}\pi) H_S U_y^{1-2}(\tfrac{1}{2}\pi) = -\delta\omega S_x^{1-2} + \sqrt{2}\omega_{1S} S_z^{1-2} - (\tfrac{4}{3}\omega_Q + \delta\omega)(S_z^{1-3} + S_z^{2-3}). \tag{3.9}$$

This Hamiltonian can be written in terms of two commuting parts:

$$H_S^T + H_{S1}^T + H_{S2}^T, \tag{3.10}$$

with

$$H_{S1}^T = \sqrt{2}\omega_{1S} S_z^{1-2} - \delta\omega S_x^{1-2}, \qquad H_{S2}^T = -(\tfrac{4}{3}\omega_Q + \delta\omega)(S_z^{1-3} + S_z^{2-3}), \tag{3.11}$$

and

$$[H_{S1}^T, H_{S2}^T] = 0. \tag{3.12}$$

The commutation relation can be verified using the general rule

$$[S_p^{i-j}, S_z^{i-k} + S_z^{j-k}] = 0, \quad p = x, y, z. \tag{3.13}$$

From this form of H_S we see that the Hamiltonian looks like a spin-$\frac{1}{2}$ Hamiltonian H_{S1} and a remainder H_{S2}, which is orthogonal to it thermodynamically. In this particular case the 1-2 transition forms the fictitious spin-$\frac{1}{2}$ system. The Hamiltonian H_{S1} in this coordinate system consists of an rf irradiation term with an effective field strength $\sqrt{2}\omega_{1S}$ and an off-resonance term with off-resonance frequency $\delta\omega$. In this case the a^{1-2} vector of ρ behaves like a fictitious spin-$\frac{1}{2}$ magnetization vector under off resonance $\delta\omega$ and irradiation strength $\sqrt{2}\omega_{1S}$ in the 1-2 coordinate system.

Irradiation near other allowed transition ($\Delta\omega \sim -\omega_Q$)

In the case $\Delta\omega = -\omega_Q + \delta\omega$ the Hamiltonian of Eq. (3.5) is of the form

$$H_S = -\delta\omega S_z^{2-3} - \sqrt{2}\omega_{1S} S_x^{2-3} + (\tfrac{4}{3}\omega_Q + \delta\omega)(S_z^{1-2} + S_z^{1-3}) \tag{3.14}$$

and with an additional transformation it becomes

$$H_S^T = U_y^{2-3}(-\tfrac{1}{2}\pi) H U_y^{2-3}(\tfrac{1}{2}\pi) = -\delta\omega S_x^{2-3} + \sqrt{2}\omega_{1S} S_z^{2-3} + (\tfrac{4}{3}\omega_Q + \delta\omega)(S_z^{1-2} + S_z^{1-3}),$$

with

$$U_y^{2-3}(\tfrac{1}{2}\pi) = \exp(i\tfrac{1}{2}\pi S_y^{2-3}),$$

which again can be written as

$$H^T = H_{S1}^T + H_{S2}^T, \tag{3.15}$$

but now

$$H_{S1}^T = -\delta\omega S_x^{2-3} + \sqrt{2}\omega_{1S} S_z^{2-3}\,, \qquad (3.16)$$
$$H_{S2}^T = (\tfrac{4}{3}\omega_Q + \delta\omega)(S_z^{1-2} + S_z^{1-3})\,.$$

From these equations we see that the 2-3 transition forms the fictitious spin-$\frac{1}{2}$ transition and this is exactly the irradiated transition according to the definitions in Eq. (3.1).

Irradiation near center ($\Delta\omega \sim 0$)

Weak rf irradiation $\omega_{1S} \ll \omega_Q$ near the center of the spectrum of the S spins can introduce double-quantum coherence between the levels $|1\rangle$ and $|3\rangle$. In this case we would like to be able to write the Hamiltonian also in the form of Eqs. (3.10) and (3.14). In order to obtain this form it is necessary to transform H_S with the unitary operator

$$U_y^{1-3}(\tfrac{1}{2}\pi) = \exp(i\tfrac{1}{2}\pi S_y^{1-3})\,, \qquad (3.17)$$

which results in

$$U_y^{1-3}(-\tfrac{1}{2}\pi)H_S U_y^{1-3}(\tfrac{1}{2}\pi) = -2\delta\omega S_x^{1-3} + \tfrac{2}{3}\omega_Q(S_z^{1-2} - S_z^{2-3}) - 2\omega_{1S}S_x^{2-3}$$
$$= -2\delta\omega S_x^{1-3} - \omega_Q S_z^{2-3} - 2\omega_{1S}S_x^{2-3} + \tfrac{2}{3}\omega_Q(S_z^{1-2} + S_z^{1-3})\,. \qquad (3.18)$$

The actual evaluation of this transformation and a discussion about the fact that the (1-3) transition after this transformation still corresponds to the double-quantum transition, is given elsewhere.[17] An additional transformation of H_S with the unitary operator

$$U_y^{2-3}(\theta) = \exp(-i\theta S_y^{2-3})\,,$$
$$\tan\theta = 2\omega_1/\omega_Q\,, \qquad (3.19)$$

will result in

$$H_S^T = U_y^{2-3}(-\theta)U_y^{1-3}(-\tfrac{1}{2}\pi)H_S U_y^{1-3}(\tfrac{1}{2}\pi)U_y^{2-3}(\theta)$$
$$= -2\delta\omega\cos^2\tfrac{1}{2}\theta S_x^{1-3} - 2\delta\omega\sin^2\tfrac{1}{2}\theta S_x^{1-2} - (\omega_Q^2 + 4\omega_{1S}^2)^{1/2}S_z^{2-3} + \tfrac{4}{3}\omega_Q(S_z^{1-2} + S_z^{1-3})\,. \qquad (3.20)$$

With the assumptions $\delta\omega$, $\omega_{1S} \ll \omega_Q$, and $\theta \ll 1$ this tilted Hamiltonian becomes

$$H_S^T \simeq -2\delta\omega S_x^{1-3} - \tfrac{1}{2}[(\omega_Q^2 + 4\omega_{1S}^2)^{1/2} - \omega_Q]S_z^{1-3} + \tfrac{2}{3}\omega_Q(S_z^{1-2} - S_z^{2-3})$$
$$\simeq -2\delta\omega S_x^{1-3} - (\omega_{1S}^2/\omega_Q)S_z^{1-3} + \tfrac{2}{3}\omega_Q(S_z^{1-2} + S_z^{2-3})\,. \qquad (3.21)$$

This equation can be written again as

$$H_S^T = H_{S1}^T + H_{S2}^T\,, \qquad (3.22)$$

with

$$H_{S1}^T = -2\delta\omega S_x^{1-3} - (\omega_{1S}^2/\omega_Q)S_z^{1-3}\,, \qquad (3.23)$$
$$H_{S2}^T = \tfrac{2}{3}\omega_Q(S_z^{1-2} - S_z^{2-3})\,.$$

Now the (1-3) double-quantum transition forms the fictitious spin-$\frac{1}{2}$ system.

In all three cases we succeeded in representing the Hamiltonian in terms of two commuting parts, one part representing a fictitious spin-$\frac{1}{2}$ Hamiltonian. We can now apply the theory of Sec. II to describe the cross-polarization process between the I spins and the fictitious spin-$\frac{1}{2}$ transition of S. In the following subsection we give a general description of the cross polarization of all three cases and for each case we derive explicit equations for the various interesting parameters separately.

C. Cross polarization

The Hamiltonian of the $I = \frac{1}{2}$, $S = 1$ spin system during cross polarization can be defined by

$$H^T = H_I + H_{S1}^T + H_{S2}^T + H_{IS}^T\,, \qquad (3.24)$$

where H_I is defined in Eq. (2.8) and the explicit forms of H_{S1}^T and H_{S2}^T are dependent on the experimental conditions, i.e., which transition of the S spins is irradiated and monitored. H_{IS}^T is the dipole-dipole interaction between the I and S spins and the actual form of H_{IS}^T in terms of the S_p^{i-j} operators is given later for each transition separately. If we consider again the spin temperature approximation in the rotating frame, the spin density matrix has the form

$$\rho^T = Z^{-1}(1 - \gamma\beta_1 H_{S1}^T - \beta_{S2}H_{S2}^T - \beta_I H_I)\,. \qquad (3.25)$$

The temperature coefficients of β_{S1} and β_{S2} may have different values, because their two corresponding terms in ρ^T form two constants of the

motion and therefore behave independently from the thermodynamic point of view. Cross polarization occurs only between the I spins and the part of the S spins corresponding to H_{S1}. If the spin system is prepared in a state with $\beta_I \neq \beta_{S1}$, the density matrix will evolve, during proper applied irradiation fields, towards

$$\rho^T_{\text{final}} = Z^{-1}[1 - \beta_f(H_{S1} + H_I) - \beta_{S2} H_{S2}] , \tag{3.26}$$

where the final temperature coefficient is calculated in the same way as in Sec. II:

$$\beta_f = \frac{\beta_{S1} C_{S1} + \beta_I C_I}{C_{S1} + C_1} . \tag{3.27}$$

The heat capacity C_I of the I spins is defined in Eq. (2.28) and the heat capacity C_{S1} of the H_{S1} part of the S spins equals

$$C_{S1} = \frac{\partial}{\partial \beta_{S1}} [\mathrm{Tr}(\rho^T H^T_{S1})] . \tag{3.28}$$

In a cross-polarization experiment the value of β_I in the initial density matrix is prepared in the same way as described in Sec. II. Again two techniques are considered, spin locking (SL) and adiabatic demagnetization in the rotating frame (ADRF). In the thermal mixing period the rf irradiation fields on the I and the S spins must be chosen properly in order to minimize the cross-polarization time. The efficiency of cross polarization as a function of the irradiation field intensities is discussed now for the different transitions of S. In the SL case for each transition the Hartmann-Hahn condition is derived and the β_I and β_f values are evaluated. Direct and indirect detection methods are discussed as well.

D. Single-quantum ($\Delta M = 1$) polarization

Spin temperature and the Hartmann-Hahn condition

Enhancement of one of the NMR spectral lines of rare S spins in a solid can be achieved by cross polarization between the corresponding allowed single-quantum transition of the S spins and the abundant I spins. With the general description of cross polarization in the spin system with $I = \frac{1}{2}$ and $S = 1$ given in the former paragraph, we can derive easily explicit expressions for the spin temperature coefficients in our case.

We consider an SL experiment on the (1-2) transition of S and derive the modified Hartmann-Hahn condition. The total Hamiltonian of our spin system, during the thermal mixing time is given in Eq. (3.24)

$$H^T = H^T_I + H^T_{S1} + H^T_{S2} + H^T_{IS} ,$$

with H^T_I given in Eq. (2.17) and H^T_{S1} and H^T_{S2} in Eq. (3.11). The dipole-dipole interaction H^T_{IS} is obtained by tilting H_{IS} (Eq. 2.2) with the unitary operator

$$U^{1-2}_{\text{SL}} = \exp[i\tfrac{1}{2}\pi(S^{1-2}_y + I_y)] \tag{3.29}$$

and results in

$$\begin{aligned} H^T_{IS} &= (U^{1-2}_{\text{SL}})^{-1} H_{IS} U^{1-2}_{\text{SL}} \\ &= (U^{1-2}_{\text{SL}})^{-1} \left(2\sum_{iS} b_{iS} I_{zi} (S^{1-2}_{zs} + S^{1-3}_{zs} + S^{2-3}_{zs}) \right) U^{1-2}_{\text{SL}} \\ &= 2\sum_{iS} b_{iS} I_{xi} S^{1-2}_{xs} + 2\sum_{iS} b_{iS} I_{xi} (S^{1-3}_{zs} + S^{2-3}_{zs}) \\ &= H^T_{IS1} + H^T_{IS2} . \end{aligned} \tag{3.30}$$

We used Eqs. (3.3), (3.7), and (3.9) for the derivation of Eq. (3.30). U^{1-2}_{SL} is the operator which tilts simultaneously, H_I and H_S to H^T_I and H^T_S, respectively. In Fig. 5 we show a schematic representation of the single-quantum cross-polarization process. From Eq. (3.30) we see that H^T_{IS} can be divided into two commuting parts

$$[H^T_{IS1}, H^T_{IS2}] = 0 \tag{3.31}$$

and for $\delta\omega = 0$

$$\begin{aligned} &[H^T_{IS1}, H^T_{S2}] = 0 , \\ &[H^T_{IS2}, H^T_{S1}] = 0 . \end{aligned} \tag{3.32}$$

From these commutation relations it is clear, that for experiments on the (1-2) transition, only the term H_{IS1} in the dipole-dipole interaction is active during the cross-polarization process.

To evaluate the spin temperature coefficients of our spin system after an SL experiment, we per-

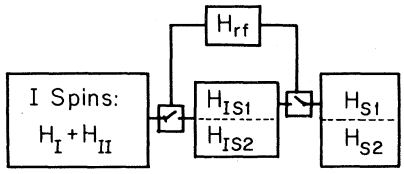

FIG. 5. Schematic representation of the cross-polarization process between a spin $I = \frac{1}{2}$ system and an allowed transition of a spin $S = 1$ system. The spin systems have Hamiltonians $H_I + H_{II}$ and $H_S = H_{S1} + H_{S2}$, respectively [Eqs. (2.15), (2.35), and (3.8)]. The part of the S-spin system, which corresponds to the allowed transition, is given by the Hamiltonian H_{S1} [Eq. (3.11)]. The dipolar interaction $H_{IS} = H_{IS1} + H_{IS2}$ between the I and the S spins is given in Eq. (3.30). H_{IS1} is the Hamiltonian of the interaction between the I spins and the allowed transition of the S spins. The Hamiltonians involved in the cross-polarization process are $H_I + H_{II}$, H_{SI} and H_{IS1} only. Cross polarization occurs if we apply the right rf irradiation field intensities ω_{II} and ω_{IS} on the I and the S spin systems, respectively; ($H_{\text{rf}} = -\omega_{II} I_x - \omega_{IS} S_x \pm \omega_Q S_z$). In the case of a spin-lock experiment this means that the Hartmann-Hahn condition in Eq. (3.34) must hold $\sqrt{2}\,\omega_{IS} = \omega_{II}$.

form a similar calculation as in Sec. II. After the preparation of the I spins, the density matrix ρ_{initial} is given again by Eq. (2.18), and thermal mixing will occur when the Hartmann-Hahn condition is fulfilled. In our case cross polarization takes place between the terms of ρ^T with

$$H_{S1}^T = -\delta\omega S_x^{1-2} + \sqrt{2}\omega_{1S} S_z^{1-2} \text{ and } H_I^T = -\omega_{1I} I_z , \tag{3.33}$$

and the corresponding Hartmann-Hahn condition becomes for $\delta\omega = 0$ (see Fig. 6)

$$\sqrt{2}\omega_{1S} = \omega_{1I} \tag{3.34}$$

and in general

$$\delta\omega^2 + 2\omega_{1S}^2 = \omega_{1I}^2 . \tag{3.35}$$

With the expression for β_f in Eq. (3.27) together with the initial value of β_I for the SL case (Eq. 2.19) we obtain

$$\beta_f = \beta_I(1 + C_{S1}/C_I)^{-1} \simeq \beta_L(\omega_{0I}/\omega_{1I})(1 - \epsilon_S) , \tag{3.36}$$

where the heat capacity C_I is given in Eq. (2.28) and the heat capacity C_{S1} equals

$$\begin{aligned} C_{S1} &= -Z^{-1}\,\mathrm{Tr}(H_{S1}^T)^2 \\ &= -Z^{-1}(\delta\omega^2 + 2\omega_{1S}^2)\,\mathrm{Tr}(S_z^{1-2})^2 \\ &= \tfrac{1}{6} N_S(\delta\omega^2 + 2\omega_{1S}^2) . \end{aligned} \tag{3.37}$$

The ratio between C_{S1} and C_I is

$$\epsilon_S = \frac{C_{S1}}{C_I} = \frac{2}{3}\frac{N_S}{N_I}\frac{\delta\omega^2 + 2\omega_{1S}^2}{\omega_{1I}^2} . \tag{3.38}$$

Insertion of β_f in the final expression for the density matrix yields

$$\rho_{\text{final}}^T = Z^{-1}[1 - \beta_L(\omega_{0I}/\omega_{1I})(1 - \epsilon_S)(-\delta\omega S_x^{1-2} + \sqrt{2}\omega_1 S_z^{1-2} - \omega_{1I} I_z) + \beta_L(\tfrac{3}{4}\omega_Q - \delta\omega)(S_z^{1-3} + S_z^{2-3})] . \tag{3.39}$$

Similar results are obtained for SL cross-polarization experiments on the (2-3) transition of the S spins.

For ADRF experiments the I-spin system is not irradiated during the thermal mixing and in order to obtain β_f from Eq. (3.27) we have to use $H_I = H_{II}$ (Eq. 2.3). The tilted frame in the ADRF case is obtained by the transformation operator

$$U_{\text{ADRF}}^{1-2} = \exp(i\tfrac{1}{2}\pi S_y^{1-2}) \tag{3.40}$$

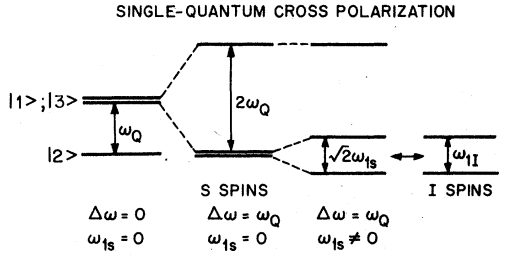

FIG. 6. Energy-level diagram of a spin $S=1$ system and a spin $I=\frac{1}{2}$ system in the rotating frame. In addition to the external magnetic field and the internal quadrupolar interaction $H_Q = \frac{1}{3}\omega_Q[S_z^2 - S(S+1)]$, rf irradiation fields are applied with $H_{\text{rf}}^S = -\omega_{1S}S_x - \Delta\omega S_z$ and $H_{\text{rf}}^I = -\omega_{II}I_x$. For $\Delta\omega = \omega_Q$ the H_{rf}^S Hamiltonian corresponds to an irradiation field at the frequency of one of the allowed transitions of the S-spin system. The energy levels of the S spins are the eigenstates of the Hamiltonian $H_Q + H_{\text{rf}}^S$ with $\Delta\omega = 0$ and $\omega_{IS} = 0$, $\Delta\omega = \omega_Q$ and $\omega_{IS} = 0$, and $\Delta\omega = \omega_Q$ and $\omega_{1S} \neq 0$. The energy levels of the I-spin system correspond also to the diagonalized Hamiltonian H_{rf}^I. In a spin-lock cross-polarization experiment the rate of the energy flow between the I and the S spins is maximum, when the S-energy difference $\sqrt{2}\omega_{1S}$ is equal to the I-energy difference ω_{II}. This is just the Hartmann-Hahn condition in Eq. (3.34).

which does not affect H_I. By replacing ω_{1I} by ω_I [Eq. (2.34)] and taking C_I from (2.40) in (3.27) we obtain the expression for β_f after the ADRF experiment.

From the expressions for β_f and ρ_{final}^T it is possible to evaluate the S-spin single-quantum signal intensities. The results of these calculations must be compared with the S-spin signal intensity after a single 90° pulse in order to obtain the enhancement factor of the cross-polarization experiment. The destruction of the I-spin signal intensity after cross polarization can also be calculated. The measurement of this destruction forms an excellent method for the detection of the efficiency of cross polarization as function of irradiation strengths, off-resonance frequencies, and time evolution of the S spins.

Signal intensities

The NMR signal intensity of the S spins after an SL experiment on the (1-2) transition can be calculated with ρ_{final}^T. This signal intensity of the (1-2) transition in the x direction is

$$\begin{aligned} M_{Sx}^{1-2} &= \sqrt{2}\,\mathrm{Tr}(\rho_{\text{final}} S_x^{1-2}) = \sqrt{2}\,\mathrm{Tr}(\rho_{\text{final}}^T S_z^{1-2}) \\ &= -Z^{-1}\beta_L \frac{\omega_{0I}}{\omega_{1I}}(1 - \epsilon_S)\sqrt{2}\omega_{1S}\,\mathrm{Tr}(S_z^{1-2})^2 \\ &= -\frac{\sqrt{2}}{6} N_S \omega_{0I}\beta_L \frac{\omega_{1S}}{\omega_{1I}}(1 - \epsilon_S) , \end{aligned} \tag{3.41}$$

where the $\sqrt{2}$ factor in (3.41) is derived from the definitions of the S_p^{i-j} operators in Eq. (3.3). In a similar way we can show that the other contributions to the S-spin signal intensities are all zero:

$$M_{S_y}^{1-2}=\sqrt{2}\,\mathrm{Tr}(\rho_{\mathrm{final}}S_y^{1-2})$$
$$=\sqrt{2}\,\mathrm{Tr}(\rho_{\mathrm{final}}^{T}S_y^{1-2})=0\,,$$
$$M_{S_x}^{2-3}=\sqrt{2}\,\mathrm{Tr}(\rho_{\mathrm{final}}S_x^{2-3})$$
$$\mathrm{Tr}[\rho_{\mathrm{final}}^{T}(S_x^{2-3}+S_x^{1-3})]=0\,, \qquad (3.42)$$
$$M_{S_y}^{2-3}=\sqrt{2}\,\mathrm{Tr}(\rho_{\mathrm{final}}S_y^{2-3})$$
$$=\mathrm{Tr}[\rho_{\mathrm{final}}^{T}(S_y^{2-3}-S_y^{1-3})]=0\,.$$

The Fourier-transform S spectrum after an SL experiment consists therefore only of the spectral line which is irradiated during the mixing time. In Fig. 7 we show a result of an SL experiment on solid deuterated benzene. We clearly see that only the signal of the cross-polarized transition appears. In the figure this signal is compared with a signal obtained after a single 90° pulse on the S spins.

To derive the enhancement of the (1-2) transition after cross polarization, with respect to the normal free-induction-decay signal after a 90° pulse, we calculate the intensity of this last signal. The intensity of the signal of the (1-2) transition after a strong 90° pulse on the S spins is

$$M_{S_x}^{1-2,0}=\sqrt{2}\,\mathrm{Tr}(\rho_{90}S_x^{1-2})$$
$$=Z^{-1}\sqrt{2}\beta_L\omega_{0S}\,\mathrm{Tr}(S_x^{1-2})^2$$
$$=\tfrac{1}{6}\sqrt{2}N_S\beta_L\omega_{0S}\,. \qquad (3.43)$$

The 90° pulse was taken in the y direction

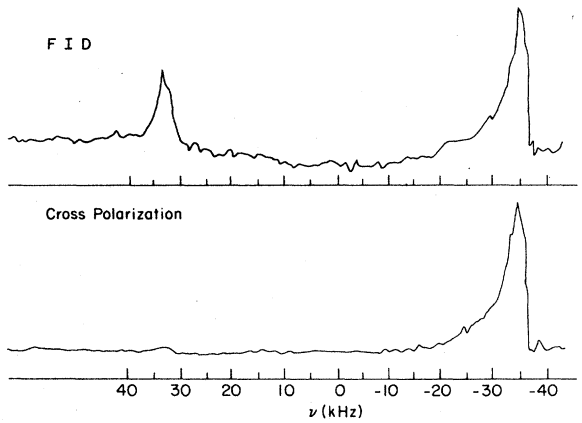

FIG. 7. Deuterium powder spectrum of solid benzene-d_1. The upper spectrum is the Fourier transform of a proton decoupled deuterium free-induction-decay signal obtained after a single strong rf pulse. This powder spectrum can be considered as if it consists only of two spectral lines at $\nu_Q=\pm 35.2$ kHz. The lower spectrum is obtained from the deuterium free-induction-decay (FID) signal after a spin-lock cross-polarization experiment on the $\nu_Q=35.2$ kHz transition. From this spectrum we see that the nonpolarized transition does not give any signal intensity, as was predicted in Eq. (3.42).

$$\rho_{90}=e^{-i(\pi/2)S_y}\rho_{\mathrm{eq}}e^{i(\pi/2)S_y}$$
$$=Z^{-1}[1-\beta_L\omega_{0S}S_x-\beta_L\omega_{0I}I_z]$$
$$=Z^{-1}[1-\sqrt{2}\beta_L\omega_{0S}(S_x^{1-2}+S_x^{2-3})-\beta_L\omega_{0I}I_z] \qquad (3.44)$$

with ρ_{eq} from Eq. (2.4).

Comparison between Eqs. (3.41) and (3.43) gives an enhancement factor

$$\frac{|M_{S_x}^{1-2}|}{|M_{S_x}^{1-2,0}|}=\frac{\omega_{0I}}{\omega_{0S}}\frac{\sqrt{2}\omega_{1S}}{\omega_{1I}}(1-\epsilon_S)$$
$$=\frac{\gamma_I}{\gamma_S}\frac{\sqrt{2}\omega_{1S}}{\omega_{1I}}(1-\epsilon_S)\,. \qquad (3.45)$$

With the Hartmann-Hahn condition and $\delta\omega=0$, the enhancement of the signal intensity $M_{S_x}^{1-2}$ is again equal to the ratio of the magnetogyric ratios of the I and S spins. This is not surprising, because the cross polarization occurs between the $I=\frac{1}{2}$ spins and the single-quantum fictitious spin-$\frac{1}{2}$ (1-2) transition of the S spins. Exactly the same results are obtained for the (2-3) transition. For an ADRF experiment on the single-quantum transitions of the S spins we obtain the same expression for $M_{S_x}^{1-2}$ as in Eq. (3.41), except that we replace ω_{1I} by ω_I.

The destruction of the I-spin signal intensity after an SL experiment on the (1-2) transition of the S spins can also be obtained easily. Similar to the derivation in Sec. II we get as in Eq. (2.48)

$$\frac{M_I^{\circ}-M_I}{M_I^{\circ}}=\epsilon_S=\frac{2}{3}\frac{N_S}{N_I}\frac{2\omega_{1S}^2+\delta\omega^2}{\omega_{1I}^2}\,. \qquad (3.46)$$

The same relative destruction is obtained for an SL experiment on the (2-3) transition of the S spins.

For an ADRF experiment the destruction of the I-spin signal is the same again as for the SL case, except that an efficiency factor η must be added to Eq. (3.46). This factor is dependent on the experimental method for the recovery of an I signal from the cooled dipole-dipole interaction reservoir of the I spins. In this article we consider the application of a 45° pulse on the I spins in order to monitor the spin temperature coefficient β_f of $\rho_{\mathrm{final}}^{T}$.

We now turn to the interesting case where the double-quantum transition of the S spins is polarized. The cross polarization between the I spins and this double-quantum transition can be used to create enhanced double-quantum coherence. Because the double-quantum coherence is independent of the quadrupolar interaction, its time behavior after cross polarization is strongly dependent on chemical shifts. Measurements of this time dependence form an alternative method for the detection of high-resolution spectra in solids.

E. Double-quantum ($\Delta M = 2$) polarization

Spin temperature and the Hartmann-Hahn condition

Cross polarization between the I spins and the double-quantum transition of the S spins can also be described with the general theory for cross polarization in the $I=\frac{1}{2}$, $S=1$ system given before. The Hamiltonian for this case is given again in Eq. (3.24) with H_I^T for the SL experiment given in (2.17). The terms H_{S1} and H_{S2} in the Hamiltonian are given in Eq. (3.23). A representation of this cross-polarization experiment is given in Fig. 8. In this case the dipole-dipole interaction term H_{IS}^T is obtained by the transformation operator

$$U_{SL}^{1-3} = \exp[i\tfrac{1}{2}\pi(S_y^{1-3} + I_y)] \exp(i\theta S_y^{2-3}), \tag{3.47}$$

$$\begin{aligned} H_{IS}^T &= (U_{SL}^{1-3})^{-1} H_{IS} U_{SL}^{1-3} \\ &= 2\sum_{is} b_{is} \cos\tfrac{1}{2}\theta S_x^{1-3} I_x \\ &\quad + 2\sum_{is} b_{is} \sin\tfrac{1}{2}\theta S_x^{1-2} I_x, \end{aligned} \tag{3.48}$$

where θ is given in Eq. (3.19). For a weak irradiation field with $\omega_{1S} \ll \omega_Q$ we have $\theta \ll 1$ and H_{IS}^T becomes

$$H_{IS}^T \simeq 2\sum_{is} b_{is} S_x^{1-3} I_x. \tag{3.49}$$

The final temperature coefficient β_f, after the thermal mixing of

$$H_{S1}^T = -2\delta\omega S_x^{1-3} - (\omega_1^2/\omega_Q) S_z^{1-3},$$

with

$$H_I = -\omega_{1I} I_z,$$

can be calculated in the same way as we did before

$$\beta_f = \beta_I (1 + C_{S1}/C_I)^{-1} \simeq \beta_I (1 - \epsilon_D). \tag{3.50}$$

The heat capacity of the double-quantum transition is

$$\begin{aligned} C_{S1} &= \frac{\partial}{\partial \beta_{S1}} \operatorname{Tr}(\rho^T H_{S1}^T) = -Z^{-1} \operatorname{Tr}(H_{S1}^T)^2 \\ &= \tfrac{1}{6} N_S (\omega_{1S}^4/\omega_Q^2 + 4\delta\omega^2) \end{aligned} \tag{3.51}$$

and the ratio ϵ_D between C_{S1} and the heat capacity of the I spins equals

$$\epsilon_D = \frac{C_{S1}}{C_I} = \frac{2}{3}\frac{N_S}{N_I}\frac{\omega_{IS}^4/\omega_Q^2 + 4\delta\omega^2}{\omega_{1I}^2}. \tag{3.52}$$

The Hartmann-Hahn condition for this case becomes with $\delta\omega = 0$ (see Fig. 9)

$$\omega_{IS}^2/\omega_Q = \omega_{1I} \tag{3.53}$$

and in general

$$\omega_{IS}^4/\omega_Q^2 + 4\delta\omega^2 = \omega_{1I}^2. \tag{3.54}$$

The density matrix after the SL cross-polarization experiment is

$$\rho_{\text{final}}^T = Z^{-1}\{1 - \beta_L(\omega_{0I}/\omega_{1I})(1 - \epsilon_D)[-2\delta\omega S_x^{1-3} - (\omega_I^2/\omega_Q) S_z^{1-3} - \omega_{1I} I_z] - \tfrac{2}{3}\beta_L \omega_Q (S_z^{1-2} - S_z^{2-3})\}. \tag{3.55}$$

For the description of ADRF experiments on the double-quantum transition we can use exactly the same arguments as were represented for the single-quantum case.

DOUBLE-QUANTUM CROSS POLARIZATION

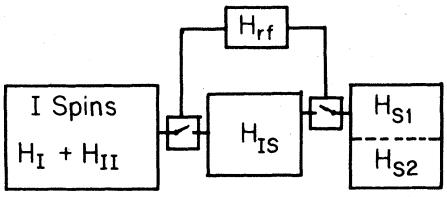

FIG. 8. Schematic representation of the cross-polarization process between a spin $I=\frac{1}{2}$ system and the double-quantum transition of a spin $S=1$ system. The spin systems have Hamiltonians $H_I + H_{II}$ and $H_S = H_{S1} + H_{S2}$, respectively [Eqs. (2.15), (2.35), and (3.23)]. The part of the S-spin system corresponding to the double-quantum transition is given by the Hamiltonian H_{S1} [Eq. (3.23)]. The whole dipolar interaction H_{IS} [Eq. (3.49)] is active during cross polarization. Cross polarization occurs if we apply the right rf irradiation field intensities ω_{1I} and ω_{1S} on the I- and S-spin systems, respectively ($H_{rf} = \omega_{1I} I_x - \omega_{1S} S_x$). In the case of a spin-lock experiment this means that the Hartmann-Hahn condition in Eq. (3.53) must hold $\omega_{IS}^2/\omega_Q = \omega_{1I}$.

Detection of the double-quantum coherence

The double-quantum coherence, created at the end of a cross-polarization experiment, cannot be measured directly. In order to transform this double-quantum coherence to single-quantum coherence, it is necessary to apply an additional 90° pulse on the S spins. To transfer the total double-quantum coherence to single-quantum coherence, this 90° pulse must be 45° out of phase with the x direction.

For the SL case on the (1-3) transition the double-quantum coherence is

$$\rho_{DQ}^T = Z^{-1}\beta_L \frac{\omega_{0I}}{\omega_{1I}}(1 - \epsilon_D)\frac{\omega_I^2}{\omega_Q} S_z^{1-3}. \tag{3.56}$$

In Appendix A the effect of this pulse on ρ_{DQ}^T is calculated for the ideal case that the irradiation intensity is much stronger than the quadrupolar interaction. In the rotating frame the result is

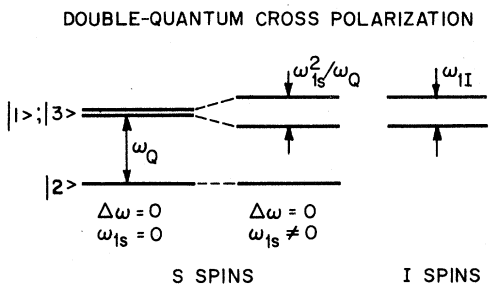

FIG. 9. Energy-level diagram of a spin $S=1$ system and a spin $I=\frac{1}{2}$ system in the rotating frame. In addition to the external magnetic field and the internal quadrupolar interaction $\{H_Q=\frac{1}{3}\omega_0[S_z^2-S(S+1)]\}$ rf irradiation fields are applied with $H_{rf}^S=-\omega_{1S}S_x$ and $H_{rf}^I=-\omega_{1I}I_x$. For ω_{1S} much smaller than the quadrupole frequency ω_Q, H_{rf}^S results in an effective irradiation of the double-quantum transition of S. The energy levels of the S-spin system are the eigenstates of the Hamiltonian $H_Q+H_{rf}^S$ with $\omega_{1S}=0$ and $\omega_{1S}\neq 0$. The energy levels of the I-spin system are the eigenstates of the Hamiltonian H_{rf}^I. In a spin-lock cross-polarization experiment the rate of the energy flow between the I spins and the S spins is maximum when the S-energy difference ω_{1S}^2/ω_Q is equal to the I-energy difference ω_{1I}. This is just the Hartmann-Hahn condition in Eq. (3.53).

$$\rho_{DQ}=\tfrac{1}{2}Z^{-1}\beta_L\frac{\omega_{0I}}{\omega_{1I}}(1-\epsilon_D)\frac{\omega_I^2}{\omega_Q}(S_y^{1-2}-S_y^{2-3}+S_x^{1-2}-S_x^{2-3}). \tag{3.57}$$

These single-quantum terms of the density matrix can be measured and give a signal intensity of

$$M_S=Z^{-1}\beta_L\frac{\omega_{0I}}{\omega_{1I}}(1-\epsilon_D)\frac{\omega_{IS}^2}{\omega_Q}. \tag{3.58}$$

This signal must be compared with the intensity of the signal after a single strong 90° pulse on the S spins

$$M_S^\circ=\mathrm{Tr}(\rho_{eq}S_z)=Z^{-1}\beta_L\omega_{0S}. \tag{3.59}$$

The ratio between the signals in Eqs. (3.58) and (3.59) becomes

$$\frac{|M_S|}{|M_S^\circ|}=\frac{\omega_{0I}}{\omega_{0S}}\frac{\omega_{IS}}{\omega_{1I}\omega_Q}(1-\epsilon_D)=\frac{\gamma_I}{\gamma_S}\frac{\omega_{1S}^2}{\omega_{1I}\omega_Q}(1-\epsilon_D). \tag{3.60}$$

From these results it is clear that the double-quantum coherence can be monitored with higher sensitivity than normal single-quantum coherences.

To follow the cross-polarization process with the double-quantum transition, we can detect again the destruction of the I-spin signal intensity after the thermal mixing period. The results for the relative destruction of the I signals are exactly the same as for the single-quantum cross-polarization case. Changing the effective irradiation field intensity of the single-quantum case to the intensity for the double-quantum case and putting ϵ_D instead of ϵ_S in Eq. (3.46) we obtain

$$\frac{M_I^\circ-M_I}{M_I^\circ}=\epsilon_D=\frac{2}{3}\frac{N_S}{N_I}\frac{\omega_{IS}^4/\omega_Q^2+4\delta\omega^2}{\omega_{1I}^2}. \tag{3.61}$$

Again, this can be used to monitor the S high-resolution double-quantum free-induction decay $[S_D(t)]$ by the method of Ref. 12. In this case $(M_I^\circ-M_I)/M_I^\circ=\epsilon_D[2-S_D(t)]$ for one contact.

In this section we showed that it is possible to obtain enhanced NMR signals from single- and double-quantum transitions by cross-polarization experiments. Direct and indirect detection methods can be used to follow the cross-polarization processes. Several experimental results of deuterium-proton cross polarization in a powder sample of benzene-d_1 will be demonstrated later. However, before we compare these experimental results with theory, we shall discuss some of the dynamical properties of cross polarization.

IV. DYNAMICS OF CROSS POLARIZATION

A. Introduction

The most important parameter concerning the dynamics of cross polarization is the rate of spin thermal mixing T_{IS}^{-1} between the I and S spins. If we know the dependence of T_{IS}^{-1} on the experimental parameters ω_{1S}, ω_{1I}, and $\Delta\omega$, then we can design and perform efficient cross polarization and signal enhancement experiments. In order for the spin system to reach thermal equilibrium, the length of the mixing time of a contact must be of the order of T_{IS}. For mixing times shorter than T_{IS}, the spin system does not reach equilibrium and the spin temperatures β_I and β_S of the I and S spins in a crystal do not become equal. In this case the values of β_I and β_S can be calculated from the rate equation, which describes the spin energy flow between the I- and S-spin systems.

In this section we calculate T_{IS}^{-1} as a function of the experimental and lattice parameters for a spin system with spins $I=\frac{1}{2}$ and $S=1$. McArthur *et al.*[14] and Demco *et al.*[15] derived expressions for T_{IS}^{-1} for the $I=S=\frac{1}{2}$ case, and we extend their theory to obtain T_{IS}^{-1} for the $I=\frac{1}{2}$, $S=1$ case. To form a theoretical basis for our extention, we first give a brief review of the $I=S=\frac{1}{2}$ case. Then the equations for the $I=S=\frac{1}{2}$ case are used in order to obtain explicit expressions for T_{IS}^{-1} for the spin system with $I=\frac{1}{2}$ and $S=1$.

B. Cross relaxation between $I=\frac{1}{2}$ and $S=\frac{1}{2}$ spins

During a cross-polarization experiment on abundant I spins and rare S spins in a solid, energy

flows from a "cold" I-spin system to a "hot" S-spin system. The rate of the energy transport is dependent on the experimental parameters and the dipolar interactions between the spins. The dipolar interaction H_{IS} between the I and S spins forms the main mechanism for this energy transfer. Due to the mutual spin flips among the I spins, this interaction H_{IS} is fluctuated. These fluctuations cause spin flips among the I and the S spins. The efficiency of the energy flow, created by this mechanism, is strongly dependent on the external applied rf fields. In the rotating frame, the I and S spins must be prepared in such a state that these mutual flips conserve energy. For example in the case of a spin-lock experiment this is accomplished by the Hartmann-Hahn condition.

It is clear from these arguments that the rate of cross relaxation T_{IS}^{-1} is dependent on the strength of the H_{IS} interaction and on the correlation function of the fluctuations of H_{IS}, caused by the dipole-dipole interaction H_{II} between the I spins. The expression for T_{IS}^{-1} in terms of these interactions was given by McArthur *et al.*[14] For a spin system with $I=\frac{1}{2}$ and $S=\frac{1}{2}$ they obtained for the cross-relaxation rate

$$T_{IS}^{-1}=\frac{1}{\mathrm{Tr}(H_{IS})^2}\int_0^\infty dt\ \mathrm{Tr}([H_{IS},H_S]e^{-i(H_S+H_I)t} \times [H_{IS},H_S]e^{i(H_S+H_I)t}). \quad (4.1)$$

From this equation we see that the rate of cross polarization is equal to the time integral of the auto correlation function of that part of H_{IS} which does not commute with H_S. This part of H_{IS} causes the fluctuations in the S-spin system and therefore governs the value T_{IS}^{-1}. Equation (4.1) was derived with the assumption that at any time during cross polarization, the I and S spins have a well defined spin temperature. The spin Hamiltonian $H=H_I+H_SH_{IS}$ for the $I=S=\frac{1}{2}$ case is given in Sec. II and its terms must be inserted in Eq. (4.1). Because the explicit forms of these terms are dependent on the type of cross-polarization experiment, we calculate the cross-relaxation rates T_{IS}^{-1} for SL and ADRF measurements separately.

SL experiments

In a spin-lock experiment the spin Hamiltonian in the rotating frame of the spin system with $I=S=\frac{1}{2}$ is given in Eq. (2.7). Because the traces in Eq. (4.1) are independent of the representation of H, the terms of the tilted Hamiltonian H^T [Eq. (2.17)] can also be inserted into the expression for T_{IS}^{-1}. The terms of the tilted Hamiltonian are

$$H_I^T=-\omega_{1I}I_z+H_{II}^T, \quad (4.2a)$$

$$H_S^T=-\omega_{1S}S_z-\Delta\omega S_x, \quad (4.2b)$$

$$H_{IS}^T=2\sum_i b_i I_{xi}S_x, \quad (4.2c)$$

$$H_{II}^T=\sum_{ij}a_{ij}(I_iI_j-3I_{xi}I_{xj}). \quad (4.2d)$$

In Eq. (4.2b) an off-resonance term is added in order to compare its effect on T_{IS} in the $I=\frac{1}{2}$, $S=\frac{1}{2}$ case with the effect of off-resonance terms in cases with $I=\frac{1}{2}$, $S=1$. The summation in Eq. (4.2c) is reduced to the I spins only, because the S spins are very low in abundance and they can be considered as single isolated spins.

If the irradiation field intensity ω_{1I} is much larger than the strength of the H_{II}^T dipolar interaction in the H^T Hamiltonian, this dipolar interaction must be truncated. Only the part of H_{II}^T which commutes with $-\omega_{1I}I_z$ (the secular part) remains and it equals

$$H_{II}^{T(0)}=-\tfrac{1}{2}\sum_{ij}a_{ij}(I_iI_j-3I_{zi}I_{zj}). \quad (4.3)$$

Before insertion of Eqs. (4.2) into (4.1) we perform an additional tilt on the Hamiltonian H^T in order to simplify the actual calculations:

$$H^{TT}=U(-\theta)H^TU(\theta), \quad (4.4)$$

with

$$U(\theta)=\exp(-i\theta S_y)$$

and

$$\tan\theta=\Delta\omega/\omega_{1S}.$$

This tilt results in the following:

$$H_I^{TT}=H_I^T, \quad (4.5a)$$

$$H_S^{TT}=-\omega_{eS}S_z, \quad (4.5b)$$

$$H_{IS}^{TT}=2\cos\theta\sum_i b_iI_{xi}S_x+2\sin\theta\sum_i b_iI_xS_z, \quad (4.5c)$$

$$H_{II}^{TT(0)}=H_{II}^{T(0)}, \quad (4.5d)$$

and

$$\omega_{eS}^2=\Delta\omega^2+\omega_{1S}^2.$$

With these equations a straightforward calculation of T_{IS}^{-1} in (4.1) yields

$$T_{IS}^{-1}=\tfrac{1}{2}\cos^2\theta M_2^S J_z(\omega_{eS}-\omega_{1I}), \quad (4.6)$$

where the second moment M_2^S equals

$$M_2^S=\frac{\mathrm{Tr}[H_{IS}^T,S_z]^2}{\mathrm{Tr}[S_z]^2} \quad (4.7)$$

and the spectral density $J_z(\omega)$ is defined by

$$J_z=\int_0^\infty dt\cos\omega t C_z(t), \quad (4.8)$$

with the autocorrelation function

$$C_x(t)=\left[\mathrm{Tr}\left(\sum_i b_i I_{zi}\right)^2\right]^{-1}\mathrm{Tr}\left[\left(\sum_i b_i I_{zi}\right)e^{-iH_{II}^{T(0)}t}\left(\sum_i b_i I_{zi}\right)e^{iH_{II}^{T(0)}t}\right]. \tag{4.9}$$

M_2^S is the second moment of the S-spin spectral line, broadened only by the dipolar interaction between the S and I spins. The auto correlation function $C_x(\tau)$ represents the fluctuations of the dipolar interaction caused by the effective part of the H_{II} interaction. The spectral density $J_x(\omega)$ gives the density of these fluctuations at frequency ω. Because the spectral density is maximum at $\omega=0$, the T_{IS}^{-1} is high when the experimental parameters ω_{1S}, $\Delta\omega$, and ω_{1I} are chosen according to the Hartmann-Hahn condition

$$\omega_e=\omega_{1I}.$$

From Eq. (4.6) we see that T_{IS}^{-1} can be calculated, if we know the experimental parameters ω_{1S}, $\Delta\omega$, and ω_{1I}, and if we evaluate M_2^S from the positions of the I and S nuclei in the sample. The functional forms of the spectral densities for SL and ADRF experiments were derived before and their values together with the other parameters govern the actual values of T_{IS}^{-1}.

ADFR experiments

The cross-relaxation rate T_{IS}^{-1} for the ADRF experiments must be calculated again from Eq. (4.1). In this case, however, the terms of the tilted Hamiltonian H^T are given in Eq. (2.37). With the addition of an off-resonance term in H_S^T and with the introduction of the tilt, defined in Eq. (4.4), the Hamiltonian is again given by the expressions in Eq. (4.2) except that $\omega_{1I}=0$. In this case H_{II}^T should not be truncated. Insertion of Eq. (4.2) in (4.1) gives for the ADRF case

$$T_{IS}^{-1}=\cos^2\theta M_2^S J_x(\omega_e), \tag{4.10}$$

where the spectral density is now given by

$$J_x(\omega)=\int_0^\infty dt\cos\omega t C_x(\tau), \tag{4.11}$$

with the auto correlation function

$$C_x(\tau)=\left[\mathrm{Tr}\left(\sum_i b_i I_{zi}\right)^2\right]^{-1}\mathrm{Tr}\left[\left(\sum_i b_i I_{zi}\right)e^{-iH_{II}^T t}\left(\sum_i b_i I_{zi}\right)e^{iH_{II}^T t}\right]. \tag{4.12}$$

Differences between the T_{IS}^{-1} values for the SL and ADRF cases are discussed at length elsewhere.[15]

The behavior of the I and S spins during cross polarization can be described by the rate equation for the energy flow between the two spin systems in terms of their spin temperatures

$$\frac{\partial}{\partial t}\beta_S=-\frac{\beta_S-\beta_I}{T_{IS}},\qquad \frac{\partial}{\partial t}\beta_I=-\frac{\epsilon(\beta_I-\beta_S)}{T_{IS}}. \tag{4.13}$$

ϵ is the ratio between the heat capacities of the S and I spins [Eq. (2.30)]. In these rate equations we neglected all spin-lattice relaxation terms. The solutions of these coupled equations give the time behavior of β_I and β_S during the thermal mixing of a CP experiment. These results can then be used to calculate the enhancements of the S-spin signal intensities and the decrease in intensity of the I-spins signals [Eqs. (2.42) and (2.48)].

After this brief description of T_{IS}^{-1} for $I=S=\frac{1}{2}$, we will now discuss the case of $I=\frac{1}{2}$ and $S=1$. The dynamics of the cross polarization of the single- and double-quantum transitions of the S spins are discussed separately.

C. Single-quantum cross relaxation between $I=\frac{1}{2}$ and $S=1$ spins

We discuss here the dynamics of cross polarization between $I=\frac{1}{2}$ spins and the (1-2) single-quantum ($\Delta M=1$) transition of the $S=1$ spins. With the concepts of fictitious spin-$\frac{1}{2}$ transitions for spins with $S=1$, described in Sec. III B, it is easy to calculate the cross-relaxation rate of this process. As was shown in Sec. III the single-quantum transition of S can be treated as a fictitious single spin-$\frac{1}{2}$ transition. The Hamiltonian H_{S1} [Eq. (3.11)], corresponding to this transition, can be considered independently from the remainder of the spin system, if we assume that $\omega_{1S}\ll\omega_Q$. The dipolar interaction H_{IS} can also be divided into two commutating terms, H_{IS1} [Eq. (3.30)] representing the interaction between the I spins and the single-quantum transition and H_{IS2} the interaction with the rest of the S system. Thus the expression for T_{IS}^{-1} in Eq. (4.1) can be used for the single-

quantum transition, if we consider only those terms in the Hamiltonian which correspond to this transition. The effective Hamiltonian for this case is given in Eqs. (3.11) and (3.30) and in the tilted frame of Eq. (3.29) we get

$$H^T = H_I^T + H_{S1}^T + H_{IS1}^T ,$$

with

$$\begin{aligned} H_{S1}^T &= \sqrt{2}\omega_{1S} S_z^{1-2} - \delta\omega S_x^{1-2} , \\ H_{IS1}^T &= 2\sum_i b_i I_{xi} S_x^{1-2} , \end{aligned} \tag{4.14}$$

and H_I^T and H_{II}^T as defined in Eq. (4.2). For convenience we perform an additional tilt on H^T with

$$\begin{aligned} H^{TT} &= U(-\theta^{1-2}) H^T U(\theta^{1-2}) , \\ U &= \exp(i\theta^{1-2} S_y^{1-2}) , \\ \tan\theta^{1-2} &= \delta\omega/\sqrt{2}\omega_{1S} , \end{aligned} \tag{4.15}$$

which results in

$$\begin{aligned} H_{S1}^{TT} &= \omega_e^{1-2} S_z^{1-2} , \\ H_{IS}^{TT} &= 2\cos\theta^{1-2} \sum_i b_i I_{xi} S_x^{1-2} \\ &\quad - 2\sin\theta^{1-2} \sum_i b_i I_{xi} S_z^{1-2} , \\ H_I^{TT} &= H_I^T , \quad H_{II}^{TT(0)} = H_{II}^{T(0)} , \end{aligned} \tag{4.16}$$

and

$$(\omega_e^{1-2})^2 = 2\omega_{1S}^2 + \delta\omega^2 .$$

For the SL and ADRF experiments we can use Eqs. (4.16) and insert them in Eq. (4.2). The results for T_{IS}^{-1} have the same form as in Eqs. (4.6) and (4.10). For the SL case we obtain

$$T_{IS}^{-1} = \tfrac{1}{2}\cos^2\theta^{1-2} M_2^{SQ} J_x(\omega_e^{1-2} - \omega_{1I}) \tag{4.17}$$

and for the ADRF case

$$T_{IS}^{-1} = \cos^2\theta^{1-2} M_2^{SQ} J_z(\omega_e^{1-2}) . \tag{4.18}$$

The spectral densities J_x and J_z are given in Eqs. (4.8) and (4.11) and are exactly the same as for the $I = S = \frac{1}{2}$ case. The second moment in Eqs. (4.17) and (4.18) is

$$M_2^{SQ} = \frac{\mathrm{Tr}[H_{IS1}^T, S_z^{1-2}]^2}{\mathrm{Tr}(S_z^{1-2})^2} . \tag{4.19}$$

M_2^{SQ} is the second moment of the (1-2) transition of the S spins due to the interaction between the S and I spins. The results of Eqs. (4.17) and (4.18) are the same as for the $I = S = \frac{1}{2}$ case. This is not surprising, because the irradiated (1-2) transition behaves exactly as a spin-$\frac{1}{2}$ transition as long as the applied rf irradiation field is not strong enough to excite the (2-3) transition also. It is clear that the same results for T_{IS}^{-1} are obtained for cross-polarization experiments on the (2-3) transition of the S spins.

D. Double-quantum cross relaxation between $I = \frac{1}{2}$ and $S = 1$ spins

Cross polarization between the $i = \frac{1}{2}$ spins and the double-quantum transition of the $S = 1$ spins can be treated in exactly the same way as in the single-quantum case. We use again the fictitious spin-$\frac{1}{2}$ character of the double-quantum transition and insert the terms of its fictitious spin-$\frac{1}{2}$ Hamiltonian in the Eq. (4.1) for T_{IS}^{-1}.

It was shown in Sec. III E that for weak irradiation fields $\omega_{1S} \gg \omega_Q$ near the Larmor frequency of the S spins, the tilted Hamiltonian corresponding to the double-quantum transition is given by

$$\begin{aligned} H^T &= H_I^T + H_{S1}^T + H_{IS1}^T , \\ H_{S1}^T &= (\omega_{1S}^2/\omega_Q) S_z^{1-3} - 2\delta\omega S_x^{1-3} , \\ H_{IS1}^T &= H_{IS}^T = \sum_i b_i I_{xi} S_x^{1-3} , \end{aligned} \tag{4.20}$$

and H_I^T and H_{II}^T are defined in Eq. (4.2).

For small ω_{1S} values the S-spin Hamiltonian H_S is again divided into two commuting parts H_{S1} and H_{S2} and the dipolar interaction H_{IS1}^T equals H_{IS}^T. As we did in the single-quantum case we apply an additional tilt on H^T and obtain

$$H^{TT} = U(-\theta^{1-3}) H^T U(\theta^{1-3}) ,$$

where

$$\begin{aligned} U(\theta) &= \exp(i\theta S_y^{1-3}) , \\ \tan\theta^{1-3} &= \delta\omega\omega_Q/\omega_{1S}^2 . \end{aligned} \tag{4.21}$$

We find

$$\begin{aligned} H_{S1}^{TT} &= -\omega_e^{1-3} S_z^{1-3} , \\ H_{IS1}^{TT} &= 4\cos\theta^{1-3} \sum_i b_i I_{xi} S_x^{1-3} \\ &\quad - 4\sin\theta^{1-3} \sum_i b_i I_{xi} S_z^{1-3} , \end{aligned} \tag{4.22}$$

where

$$(\omega_e^{1-3})^2 = \omega_{1S}^4/\omega_Q^2 + 4\delta\omega^2 .$$

Insertion of (4.22) into (4.1) results for the SL case in

$$T_{IS}^{-1} = \tfrac{1}{2}\cos^2\theta^{1-3} M_2^{DQ} J_x(\omega_e^{1-3} - \omega_{1I}) \tag{4.23}$$

and for the ADRF case

$$T_{IS}^{-1} = \cos^2\theta^{1-3} M_2^{DQ} J_z(\omega_e^{1-3}) . \tag{4.24}$$

The spectral density functions J_x and J_z are again the same as in Eqs. (4.8) and (4.11). M_2^{DQ} is given by

$$M_2^{DQ} = \frac{\mathrm{Tr}[H_{IS}^T, S_z^{1-3}]^2}{\mathrm{Tr}(S_z^{1-3})^2}$$

and is equal to the second moment of the Fourier-transform double-quantum spectrum of the S spins, broadened by the heteronuclear dipolar interaction H_{IS}.

The ratio between the cross-relaxation rates of the single-quantum and the double-quantum transition equals

$$\frac{(T_{IS}^{-1})_{DQ}}{(T_{IS}^{-1})_{SQ}}=\frac{\cos^2\theta^{1-3}}{\cos^2\theta^{1-2}}\frac{M_2^{DQ}}{M_2^{SQ}}\,. \tag{4.25}$$

The ratio between the second moments can easily be calculated

$$\frac{M_2^{DQ}}{M_2^{SQ}}=\frac{\mathrm{Tr}(4\sum_i S_z^{1-3}I_{xi},S_z^{1-3})^2}{\mathrm{Tr}(2\sum_i b_i S_z^{1-2}I_{xi},S_z^{1-2})^2}=4\,. \tag{4.26}$$

From this ratio it follows that the width of the double-quantum spectral lines, broadened by H_{IS}, are twice as large as the width of the single-quantum lines.

To examine the theory of this section and Sec. III we performed some proton-deuterium cross-polarization experiments on solid benzene-d_1. The experimental results are shown in Sec. V and are compared with the results of this section and Sec. III. The Hartmann-Hahn condition is checked by single- and double-quantum cross-polarization experiments as a function of rf irradiation field strengths and off-resonance frequencies. The efficiency of cross polarization is studied for SL and ADRF measurements, and the cross-relaxation time T_{IS} is evaluated.

V. EXPERIMENTS

A. Introduction

The experiments were performed on a powder sample of monodeutero-benzene. The spin-lattice relaxation time of this material is relatively short (~ 0.5 sec) and it is convenient to use this sample for the accumulation of free-induction-decay signals after cross-polarization experiments. The deuterium quadrupole interaction frequency of benzene-d_1 equals $2\nu_Q=70.4$ kHz and the maxima in its powder spectrum are at $\nu_Q=\pm35.2$ kHz. In this paper, it is sufficient to consider only the two peaks at ±35.2 kHz for the interpretation of our experimental results, and to ignore the rest of the powder spectrum. If, however, the deuterium enhanced proton-NMR-signal intensities were used to obtain information on the chemical shifts of the deuterium atom, the whole spectrum should be taken into account.

All measurements were done on a home built spectrometer with a static magnetic field of 25 kG. The sample was kept at a constant temperature of −35°C by a temperature-regulated nitrogen gas stream.

Cross polarization in solid benzene-d_1 occurs between the protons ($I=\frac{1}{2}$) and the deuterons ($S=1$). The efficiency of the cross-polarization experiments as a function of rf irradiation field intensities and of off-resonance frequencies was measured through the detection of the relative destruction of the proton-signal intensities after the thermal mixing. This indirect detection method is very sensitive and makes it possible to check the Hartmann-Hahn conditions experimentally. Direct detection of the deuterium signals is used to examine the signal enhancements which are caused by cross polarization, and to measure the cross-relaxation rate T_{IS}^{-1}.

B. Indirect detection

In this subsection we show some experimental results of the destruction of the proton line intensity as a function of the rf irradiation field intensities $\nu_{1I}=\omega_{1I}/2\pi$ and $\nu_{1S}=\omega_{1S}/2\pi$, and the off-resonance frequencies $\Delta\nu=\delta\omega/2\pi$.

The dependence on rf intensities

The relative destruction of the proton-spectrum intensity after a cross-polarization experiment can be calculated from the maximum possible destruction, given in Eqs. (3.46) and (3.61), and the cross-relaxation time T_{IS}. For a spin-lock experiment on the (1-2) single-quantum (SQ) transition of the deuterium atom, the relative destruction as function of the experimental mixing time t can be represented by

$$\begin{aligned}d_{SQ}(\nu_{1S},\Delta\nu)&=\frac{M_I^0-M_I}{M_I^0}(1-e^{-t/T_{IS}})\\&=\epsilon_S(1-e^{-t/T_{IS}}),\end{aligned} \tag{5.1}$$

where T_{IS} is given in Eq. (4.17). For t values much smaller than T_{IS}, we can take $\exp(-t/T_{IS})\simeq 1-t/T_{IS}$ and we get [with θ^{1-2} from Eq. (4.15)]

$$\begin{aligned}&d_{SQ}(\nu_{1S},\Delta\nu)\\&\simeq\epsilon_S t T_{IS}\\&=\frac{2}{3}\frac{N_S}{N_I}\frac{\Delta\nu^2+2\nu_{1S}^2}{\nu_{1I}^2}\tfrac{1}{2}t\cos^2\theta^{1-2}M_2^{SQ}J_x(\nu_e^{1-2}-\nu_{1I})\\&=\frac{1}{3}\frac{N_S}{N_I}\frac{2\nu_{1S}^2}{\nu_{1I}^2}tM_2^{SQ}J_x(\nu_e^{1-2}-\nu_{1I})\,.\end{aligned} \tag{5.2}$$

For a spin-lock experiment on the double-quantum transition we get in the same way [with T_{IS}^{-1} from Eq. (4.23) and θ^{1-3} from Eq. (4.21)]

$$d_{SQ}(\nu_{1S},\Delta\nu)=\frac{1}{3}\frac{N_S}{N_I}\frac{\nu_{1S}^4}{\nu_Q^2\nu_{1I}^2}tM_2^{DQ}J_x(\nu_{eS}^{1-3}-\nu_{1I})\,. \tag{5.3}$$

With $\Delta\nu=0$ and the Hartmann-Hahn conditions

$\sqrt{2}\nu_{1S} = \nu_{1I}$ for the single-quantum and $\nu_{1S}^2/\nu_Q = \nu_{1I}$ for the double-quantum case, the ratio between d_{DQ} and d_{SQ} equals

$$\frac{d_{DQ}}{d_{SQ}} = \frac{M_2^{DQ}}{M_2^{SQ}} = 4. \tag{5.4}$$

This shows that the destruction of the I (proton) spins for the double-quantum case is larger than for the single-quantum case. Furthermore the maximum destruction is obtained when the Hartmann-Hahn condition is fulfilled and $J_x(0) = 1$. Comparison between the widths of d_{DQ} and d_{SQ} as functions of ν_{1S} predicts that d_{DQ} is broader than d_{SQ}. This can be understood best if we take for $J_x(\nu)$[15] a Gaussian function $e^{-\nu^2/\nu_c^2}$.

The destruction spectra d_{SQ} and d_{DQ} for the ADRF experiments can also be derived from Eq. (5.2) with T_{IS} from Eqs. (4.18) and (4.24). The results for $t \ll T_{IS}$ are

$$d_{SQ}(\nu_{1S}, \Delta\nu) = \frac{2}{3}\frac{N_S}{N_I}\frac{2\nu_{1S}^2}{\nu_I^2} tM_S^{SQ} J_x(\nu_e^{1-2}) \tag{5.5}$$

and

$$d_{DQ}(\nu_{1S}, \Delta\nu) = \frac{2}{3}\frac{N_S}{N_I}\frac{\nu_{1S}^4}{\nu_I^2\nu_Q^2} tM_S^{DQ} J_x(\nu_e^{1-3}). \tag{5.6}$$

Here it is difficult to predict for what value of ν_{1S} the maximum destruction is obtained. If we take for the spectral density function $J_x(\nu)$[15] an exponential function $e^{-\nu/\nu_c}$, it is clear that the width of d_{DQ} as a function of ν_{1S} is larger than the width of d_{SQ} and that the maximum in d_{DQ} is larger than the maximum in d_{SQ}.

In Fig. 10 we show the relative destruction as a function of ν_{1S} of the proton line intensity after a spin-lock experiment on the single- and double-quantum transitions of deuterium in benzene-d_1. The mixing time in these experiments was $t = 15$ msec, which is much smaller than the T_{IS} value for this compound. The applied proton rf irradiation intensity was equal to $\nu_{1I} = 10$ kHz. Maximum destruction for the single-quantum case is obtained when $\nu_{1S} = 7$ kHz. This should be equal to $2^{-1/2}\nu_{1I} = 7.1$ kHz, according to the Hartmann-Hahn condition [Eq. 3.34)]. Thus agreement is good. In the double-quantum case the maximum destruction occurs at $\nu_{1S} = 19$ kHz and this must be compared with $(\nu_Q\nu_{1I})^{1/2} = 19.2$ kHz [Eq. (3.53)]. Again, these experimental results are in excellent agreement with the theory. The results of Fig. 10 show that the maximum single-quantum destruction is smaller than for the double-quantum destruction and that the destruction spectrum for the double-quantum case is wider than for the single-quantum case. This is in agreement with the discussions given above.

The proton destruction spectra for ADRF experiments on the single- and the double-quantum deuterium transitions are shown in Fig. 11. In these experiments we took for the mixing time $t = 50$ msec. This value is of the order of T_{IS} and therefore we measure a larger destruction than in Fig. 10. In the ADRF case we see again that the $d_{SQ}(\nu_{1S})$ spectrum is narrower than $d_{DQ}(\nu_{1S})$.

In Fig. 12 SL experiments on the double-quantum transition are demonstrated for two different values of the proton rf irradiation strength. The agreement of these results with the double-quantum theoretical Hartmann-Hahn condition, indicated by arrows, is excellent.

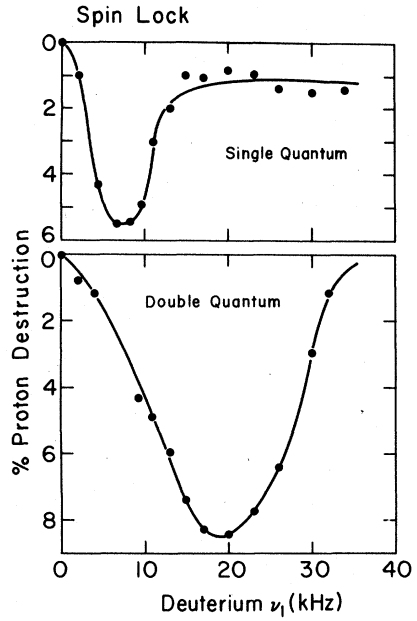

FIG. 10. The relative destructions of the proton signal intensity $(1 - M_S/M_S^0)$ (100%) of solid benzene-d_1 after spin-lock cross-polarization experiments (Fig. 2) between the protons and the deuterium nuclei in this sample. The destruction is measured as a function of the rf irradiation field strength ν_{1S} on the S spins. The rf field strength $\nu_{1I} = 10$ kHz on the protons is kept constant. The mixing time of these experiments was $t = 15$ msec. The upper graph is obtained by the irradiation of the allowed transition of the deuterium nuclei at $\nu_Q = 35.2$ kHz. The lower graph is obtained by irradiation of the deuterium nuclei at their Larmor frequency. A discussion of these results is given in the main text.

The dependence on off-resonance frequencies

We now present experimental results for the proton destruction spectra as a function of the off-resonance frequency values $\Delta\nu$. In Fig. 13 $d_{DQ}(\Delta\nu)$ is measured for different values of ν_{1S} and ν_{1I} in a spin-lock experiment. The results for the maxima in the destruction are in full agree-

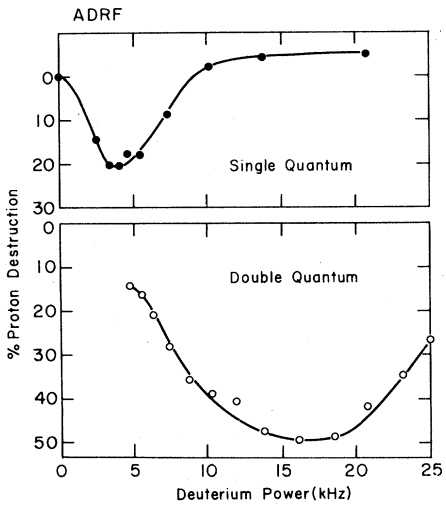

FIG. 11. The relative destructions of the proton signal intensity $(1-M_S/M_S^0)$ (100%) of solid benzene-d_1 after ADRF cross-polarization experiments (Fig. 2) between the protons and the deuterium nuclei in this sample. The destruction is measured as function of the rf irradiation field strength ν_{1S} on the S spins. The mixing time of these experiments was $t=50$ msec. The upper graph is obtained by the irradiation of the allowed transition of the deuterium nuclei at $\nu_Q=35.2$ kHz. The lower graph is obtained by irradiation at the deuterium Larmor frequency. A discussion of these results is given in the main text.

ment with the Hartmann-Hahn condition of Eq. (3.54). The numerical calculations are given in the figure caption.

The destruction spectrum $d_{DQ}(\Delta\nu)$ for an SL and an ADRF experiment are again shown in Figs. 14

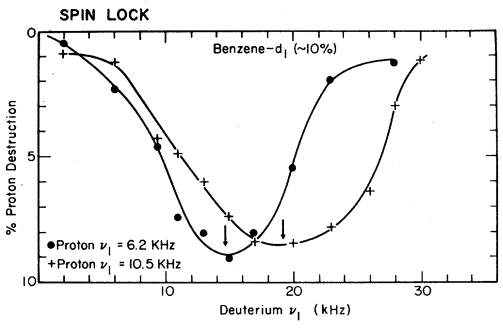

FIG. 12. Relative destructions of the proton signals of solid benzene-d_1 after cross-polarization spin-lock experiments on the deuterium double-quantum transition. The destructions were measured as function of the deuterium irradiation field strength ν_{1S} for two constant values of the proton irradiation field intensity. According to the Hartmann-Hahn condition $\nu_{1S}^2/\nu_Q=\nu_{1I}$ the maximum destruction is expected for $\nu_{1I}=6.2$ kHz at $\nu_{1S}=14.8$ kHz and for $\nu_{1I}=10.5$ kHz at $\nu_{1S}=19.2$ kHz. This is in excellent agreement with the experimental results.

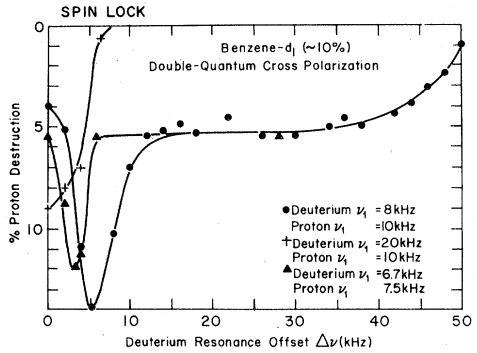

FIG. 13. Relative destructions of the proton signal intensity $(1-M_S/M_S^0)$ (100%) of solid benzene-d_1 after spin-lock cross-polarization experiments (Fig. 2) between the protons and the deuterium nuclei in this sample. The destructions are measured as function of the off-resonance frequency $\Delta\nu$ of the deuterium irradiation field. The rf field intensities ν_{1S} and ν_{1I} on the S- and the I-spin systems, respectively, were kept constant. $\Delta\nu$ was measured from the deuterium Larmor frequency. According to the Hartmann-Hahn condition $\nu_{1S}^4/\nu_Q^2+4\Delta\nu^2=\nu_{1I}^2$ the expected maxima in the destruction spectra are for $\nu_{1S}=8$ kHz and $\nu_{1I}=10$ kHz at $\Delta\nu=4.9$ kHz and for $\nu_{1S}=6.7$ kHz and $\nu_{1I}=7.5$ kHz at $\Delta\nu=3.7$ kHz. For the values $\nu_{1S}=20$ kHz and $\nu_{1I}=10$ kHz the Hartmann-Hahn condition can not be fulfulled and the maximum destruction is expected at $\Delta\nu=0$. The agreement between experiment and theory is excellent.

and 15. However, in these figures $d_{DQ}(\Delta\nu)$ is measured for positive and negative values of $\Delta\nu$. The experimental results show a marked asymmetry in $d_{DQ}(\Delta\nu)$ for opposite signs of $\Delta\nu$.[20] The experimental parameters for the spin-lock case in Fig. 14 are $\nu_{1S}=8$ kHz and $\nu_{1I}=11$ kHz and the maximum destruction is obtained at $\Delta\nu\simeq\pm5$ kHz. This value for $\Delta\nu$ gives together with ν_{1S} the effective frequency (in kHz)

$$\nu_e^{1-2}=[4\Delta\nu^2+\nu_{1S}^2/\nu_Q^2]^{1/2}=11\,,$$

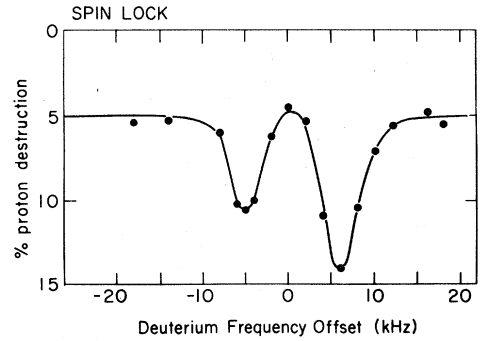

FIG. 14. The experiment in Fig. 13 with $\nu_{1S}=8$ kHz and $\nu_{1I}=10$ kHz is repeated here for positive and negative values of $\Delta\nu$. The asymmetry in the destruction spectrum is discussed in the main text.

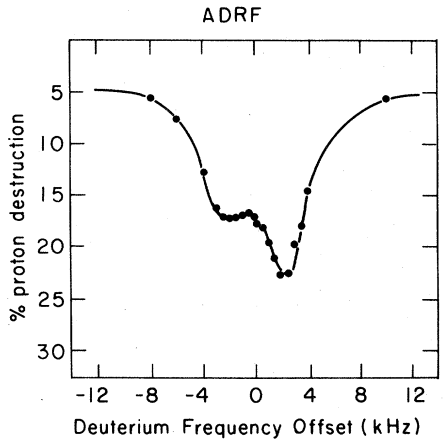

FIG. 15. Relative destructions of the proton signal intensity of solid benzene-d_1 after ADRF cross-polarization experiments. The destructions are measured as function of the off-resonance frequency $\Delta\nu$ of the deuterium irradiation field. The asymmetry of the destruction spectrum for positive and negative $\Delta\nu$ values is discussed in the main text.

which is equal to ν_{1I}.

The asymmetry in $d_{DQ}(\Delta\nu)$ can be explained,[20] if we take into account the initial condition of the deuterium-spin density matrix, before cross polarization occurs. In all cases of Sec. III, we assumed that the initial S-spin temperature coefficient β_{S1} is zero. This assumption is justified if the direction of effective rf irradiation field in the rotating frame on the S spins is perpendicular to the direction of the Zeeman field, $\delta\omega \simeq 0$. Then, at the moment the irradiation field is applied, the S spins are in a state defined by

$$\rho_{eq,S} = Z^{-1}(1+\beta_L\omega_{0S}S_z) = Z^{-1}(1+2\beta_L\omega_{0S}S_z^{1-3}) \tag{5.7}$$

and the effective irradiation Hamiltonian on the double-quantum transition [Eq. (3.23)] is

$$H_{S1} = (\omega_{1S}^2/\omega_Q)S_x^{1-3}. \tag{5.8}$$

According to the spin temperature approximation in the rotating frame, the initial S-spin density matrix is then equal to

$$\rho_{initial} = Z^{-1}(1-\beta_{S1}H_{S1}) = Z^{-1}. \tag{5.9}$$

However, if the irradiation field is not perpendicular to the Zeeman field and

$$H_S = (\omega_{1S}^2/\omega_Q)S_x^{1-3} - 2\delta\omega S_z^{1-3} \tag{5.10}$$

the initial S-spin density matrix becomes

$$\rho_{initial} = Z^{-1}[1+(2\delta\omega/\omega_e^{1-3})2\omega_{0S}\beta_L H_S], \tag{5.11}$$

where ω_e^{1-3} is defined in Eq. (4.22). Physically, this means that the S spin begins with a slight positive or negative polarization (temperature) dependency on whether we are above or below resonance. The initial value for β_{S1} is thus different from zero and equals

$$\beta_{S1} = -\frac{4\delta\omega\omega_{0S}}{(\omega_e^{1-3})^2}\beta_L. \tag{5.12}$$

The final spin temperature coefficient β_f in Eq. (3.50) must be modified and becomes

$$\beta_f = \frac{\beta_I C_I + \beta_{S1}C_{S1}}{C_I + C_{S1}} \simeq \beta_I(1-\epsilon_D) + \beta_{S1}\epsilon_D. \tag{5.13}$$

Now the relative destruction d_{DQ} must be calculated from Eq. (2.48) and gets the form

$$d_{DQ}(\Delta\nu) = \frac{\beta_I - \beta_f}{\beta_I}(1-e^{-t/T_{IS}}) = \epsilon_D\left(1-\frac{\beta_{S1}}{\beta_I}\right)(1-e^{-t/T_{IS}}). \tag{5.14}$$

Insertion of Eq. (5.12) in Eq. (5.14) results in

$$d_{DQ}(\Delta\nu) = \epsilon_D\left(1+\frac{4\Delta\nu\nu_{0S}}{(\nu_e^{1-3})^2}\frac{\nu_{1I}}{\nu_{0I}}\right)(1-e^{-t/T_{IS}}), \tag{5.15}$$

where we used the expression for β_I from Eq. (2.19) and in general $\nu = \omega/2\pi$. With the Hartmann-Hahn condition $\nu_e^{1-3} = \nu_{1I}$ we obtain

$$d_{DQ}(\Delta\nu) = \epsilon_D\left(1+\frac{4\Delta\nu}{\nu_e^{1-3}}\frac{\gamma_S}{\gamma_I}\right)(1-e^{-t/T_{IS}}). \tag{5.16}$$

The ratio between the values of d_{DQ} for positive and negative $\Delta\nu$'s is

$$\frac{d_{DQ}(\Delta\nu)}{d_{DQ}(-\Delta\nu)} = \frac{\gamma_I\nu_e^{1-3} + 4\gamma_S\Delta\nu}{\gamma_I\nu_e^{1-3} - 4\gamma_S\Delta\nu}. \tag{5.17}$$

This ratio equals 1.6 for the experimental parameters of Fig. 14. The experimental result for this ratio is 1.5.

For the ADRF case in Fig. 15 we obtain the same asymmetry in $d_{DQ}(\Delta\nu)$ as for the SL case. The rf irradiation intensity on the deuterons in this experiment is $\nu_{1S} = 14.7$ kHz and the experimental values for the maximum destruction are $\Delta\nu = \pm 3$ kHz. Insertion of these values in Eq. (5.17) results in a value of 1.5 for the ratio between the maxima. The experimental value equal is 1.4.

C. Cross-polarization dynamics

Until now we assumed that for all our experiments the spin-lattice relaxation times of the proton and the deuterium spins were much longer than the experimental mixing time t. In these cases it is sufficient to describe the spin temperature coefficients of these I and S spins by the rate equations given in Eq. (4.13). However, if we monitor the behavior of the spin system during cross polarization for long mixing times, these equations must

be extended. In this subsection we consider an ADRF experiment on the double-quantum transition. We show that from the deuterium signal intensity, as a function of the mixing time, it is possible to obtain the value of T_{IS}. These experiments also measure the value of the ratio ϵ_D between the spin heat capacities of the double-quantum deuterium transition and the protons.

The spin-lattice relaxation time for the deuterium ($S=1$) during an ADRF experiment is $T_{1\rho}$. This is the relaxation time of the deuterons during a spin-lock experiment on their double-quantum transition.[3] The relaxation time of the protons T_{1D} equals the relaxation time of the protons ($I=\frac{1}{2}$) after an adiabatic demagnetization in the rotating frame of these nuclei. Taking into account the relaxation times, the rate equation for the spin temperature coefficients β_I and β_S are given by[19]

$$\frac{d}{\partial t}\beta_I = \frac{-\epsilon_D(\beta_I-\beta_{S1})}{T_{IS}} - \frac{(\beta_I-\beta_L)}{T_{1D}},$$
$$\frac{\partial}{\partial t}\beta_{S1} = \frac{-(\beta_{S1}-\beta_I)}{T_{IS}} - \frac{(\beta_{S1}-\beta_L)}{T_{1\rho}}. \tag{5.18}$$

The solution of these coupled equations is calculated in Appendix B and with the initial conditions for the spin temperature coefficients $\beta_I(0)\neq 0$ and $\beta_{S1}(0)=0$ it becomes

$$\beta_{S1}(t)=\beta_I(0)g(t)=(\omega_{0I}/\omega_I)\beta_L g(t), \tag{5.19}$$

with $g(t)$ given in Appendix B. The corresponding density matrix of the S spins can be represented by Eq. (3.56)

$$\rho_{DQ}(t)=Z^{-1}[1-\beta_{S1}(t)H_{S1}]$$
$$=Z^{-1}[1+\beta_{S1}(t)(\omega_{1S}^2/\omega_Q)S_x^{1-3}]$$
$$=Z^{-1}[1+\beta_L\omega_{0I}(\omega_{1S}^2/\omega_Q)/\omega_I S_x^{1-3}g(t)]. \tag{5.20}$$

The time behavior of $\beta_{S1}(t)$ can be monitored by measuring the S-spin signal intensity after cross polarization as a function of t. Before we present the experimental result of the deuterium signal intensity in the ADRF experiment we show how the $T_{1\rho}$ and T_{ID} relaxation times were measured.

$T_{I\rho}$ experiment

The $T_{1\rho}$ relaxation time of the deuterium spins can be measured by a double-quantum spin-lock experiment.[3] In such an experiment the spins are locked at the effective rf irradiation field of the double-quantum transition by a 45° phase shift on this rf field. In our case we obtained the same result by a cross polarization of the deuterium double-quantum transition with the protons. In Fig. 16 the experimental scheme for this measurement is represented. The deuterium spins are polarized by an ADRF experiment and after the

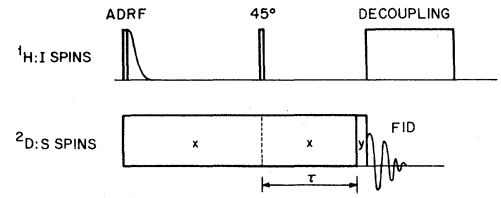

FIG. 16. The pulse cycle used for the measurement of the rotating-frame spin-lattice relaxation time $T_{1\rho}$ of the deuterium ($S=1$) double-quantum transition. This cycle starts with the polarization of the deuterium double-quantum transition by an ADRF cross-polarization experiment (Fig. 2). At the end of the cross-polarization period the proton dipolar order is destroyed by a 45° pulse and the decay of the enhanced and spin-locked deuterium double-quantum coherence is monitored as a function of the rf irradiation time τ. The double-quantum coherence is measured by applying an additional 90° out of phase rf pulse on the deuterium spins and by detecting the intensity of the proton decoupled deuterium free-induction-decay signal.

mixing time the proton dipolar order is destroyed by a 45° pulse. After this pulse the double-quantum coherence of the deuterons is spin locked and will decay with a time $T_{I\rho}$ to zero. This decay can be monitored by measuring the deuterium signal after τ sec with an additional detection pulse. The result of this experiment is shown in Fig. 17 and the value of $T_{1\rho}$ obtained, is $T_{1\rho}=43$ msec.

T_{ID} experiment

The proton T_{1D} relaxation time is measured by an ADRF experiment without applying an rf field on the deuterium nuclei. The recovery of the dipolar order of the protons is measured with a 45° pulse. The proton signal intensity after this pulse is monitored as a function of the delay time between this pulse and the ADRF pulse. The experimental result is given in Fig. 18 and $T_{1D}=300$ msec.

T_{IS} measurement

The relative deuterium signal intensity as a func-

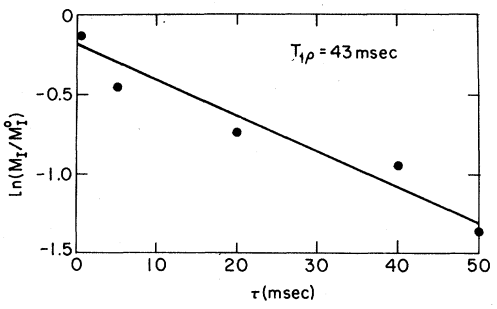

FIG. 17. Experimental result of the $T_{1\rho}$ measurement described in Fig. 16. Each point in this figure was obtained by an accumulation of many individual measurements of the deuterium signal. The obtained value of $T_{1\rho}$ is 43 msec.

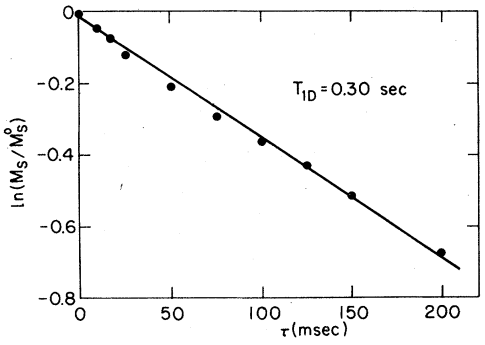

FIG. 18. The measurement of the proton local field spin-lattice relaxation time T_{1D} of solid benzene-d_1. The points in this graph are the relative proton signal intensities M_I/M_I^0 as function of the time τ between the creation of proton dipolar order by an ADRF pulse sequence (Fig. 2) and the transformation of this order to a measurable signal by a 45° pulse. From these measurements we get T_{1D} = 300 msec.

tion of the mixing time in a cross-polarization ADRF experiment is represented in Fig. 19. The experimental parameter was equal to $\nu_{1S} = 17.2$ kHz and the irradiation field was applied at resonance. This corresponds to the maximum destruction in Fig. 12. The intensities are measured after the application of an additional rf pulse with $\nu_{1S} = 17.2$ kHz. In the experiment this pulse was 90° out of phase with the mixing pulse; the maximum signal intensity which can be obtained in this case is proportional to half of the double-quantum coherence (see Appendix A). The relative intensity is therefore given in analogy with Eq. (3.60) by

$$\frac{M_S}{M_S^0} = \frac{1}{2}\frac{\mathrm{Tr}[\rho_{DQ}(t) S_x^{1-3}]}{\mathrm{Tr}(\rho_{eq} S_z)} = \tfrac{1}{2}\eta \frac{\omega_{0I}}{\omega_{0S}} \frac{\omega_{1S}^2}{\omega_I \omega_Q} g(t). \quad (5.21)$$

The experimental result of Fig. 19 together with

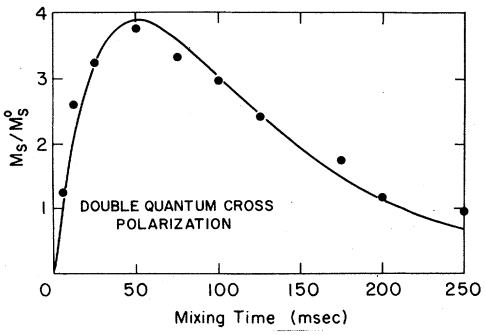

FIG. 19. The relative deuterium signal intensities M M_S/M_S^0 of solid benzene-d_1 as function of the mixing time of an ADRF cross-polarization experiment (Fig. 2) on the protons and the deuterons in this sample. The points in this figure are the experimental results and the solid line is the best-fit curve according to Eq. (5.21) through these points. The adjusted parameters in the best-fit procedure were T_{IS} and ϵ_D. The results for these parameters are $T_{IS} = 77.6$ msec and $\epsilon_D = 0.85 \pm 0.05$.

the values of T_{1D} and $T_{1\rho}$ must be compared with Eq. (5.21). A computer program was written to minimize the deviation between the experimental and theoretical result by changing the parameters ϵ_D and T_{IS}. The results of this calculation with $\eta = 0.95$ are $\epsilon_D = 0.85 \pm 0.05$ and $T_{IS} = 77.6$ msec. Insertion of these values in Eq. (5.22) results in the solid line in Fig. 19. To compare the obtained value of ϵ_D with its theoretical value, we calculated ϵ_D from Eq. (3.52) with $N_S/N_I = 0.2$ and replaced ω_{1I} by ω_I. The local field strength ω_I in frequency units of the protons was calculated from the linewidth δ_p of the proton spectrum of benzene-d_1. Assuming a Gaussian shape for this line, the ω_I value was taken as $\omega_I = \delta_p/1.18 = 2.75$ kHz and $\epsilon_D = 1.18$. This is in reasonable agreement with the experimental value 0.85.

VI. SUMMARY

The motivation of this paper has been to provide a theoretical framework and experimental results for various cross-polarization experiments between abundant $I = \frac{1}{2}$ and rare $S = 1$ spins. In particular, cross polarization between the $I = \frac{1}{2}$ and the S double-quantum transition has been treated. The double-quantum transition has previously been shown to be extremely useful for high-resolution ^{2}D and ^{14}N NMR in solids and the results of the present experiments indicate that such spectroscopy can also be done with very good sensitivity. The theory for cross-polarization thermodynamics and dynamics between $I = \frac{1}{2}$ and $S = 1$ was developed for both spin locking and adiabatic demagnatization in the rotating frame. This is a generalization of the familiar $I = S = \frac{1}{2}$ case. When $\omega_1 \ll \omega_Q$ a modified Hartmann-Hahn condition for the simplest case of double-quantum cross polarization $\omega_{1S}^2/\omega_Q = \omega_{1I}$ emerges. Experiments were performed, showing the validity of the approach both for the thermodynamics and dynamics of the cross-polarization process for double-quantum transitions. By an indirect detection the double-quantum free-induction decay of $S = 1$ can be mapped point by point. Such further experiments on ^{2}D and ^{14}N and other nuclei are under way.[21]

ACKNOWLEDGMENT

This work was supported by the Division of Materials Sciences, Office of Basic Sciences, U. S. Department of Energy. Partial support for S. V. was provided by a grant from the United States–Israel Binational Science Foundation, Jerusalem, Israel.

APPENDIX A

To transfer the total double-quantum coherence after cross polarization

$$\rho_{DQ} = a_z^{1-3} S_x^{1-3} \tag{A1}$$

to single-quantum coherence, we apply a strong 90° pulse $\omega_{1S} \gg \omega_{1Q}$ on the S spins, 45° out of phase with the mixing pulse. In this Appendix we calculate the effect of this pulse on ρ_{DQ} and we evaluate the signal intensity measured after this pulse.

The Hamiltonian of the rf pulse in the rotating frame with $\omega_{1S} \gg \omega_Q$ is

$$H_p = -(1/\sqrt{2})\omega_{1S}(S_x + S_y). \tag{A2}$$

The effect of a τ_p second pulse with $\omega_{1S}\tau_p = \pi/2$ on ρ_{DQ} is calculated by

$$\rho_{DQ}^{90} = P^{-1}\rho_{DQ}P, \tag{A3}$$

with

$$P = e^{iH_p\tau_p} = e^{-i\pi/2\sqrt{2}(S_x+S_y)}. \tag{A4}$$

In the actual calculation we make use of the commutation relations in Eq. (2.6) of Ref. 17. The expression for ρ_{DQ}^{90} is obtained as follows:

(1) Transfer ρ_{DQ} and $H_p\tau_p$ with

$$U_z = \exp(-i\tfrac{1}{4}\pi S_z) = \exp(-i\tfrac{1}{2}\pi S_z^{1-3}) \tag{A5}$$

and obtain

$$\rho_{DQ}^{T} = U_z^{-1}\rho_{DQ}U_z = -a_x^{1-3}S_y^{1-3}, \tag{A6}$$

$$H_p^T\tau_p = -\frac{\pi}{2}S_x = -(\pi/\sqrt{2})(S_x^{1-2} + S_x^{2-3}). \tag{A7}$$

(2) Perform an additional transformation with

$$U_y^{1-3} = \exp(-i\tfrac{1}{2}\pi S_y^{1-3}) \tag{A8}$$

and use Eq. (2.9) in Ref. 17:

$$\rho_{DQ}^{TT} = \rho_{DQ}^{T}, \tag{A9}$$

$$H^{TT}\tau_p = (U_y^{1-3})^{-1}H_p^T U_y^{1-3}\tau_p = -\pi S_x^{1-2}. \tag{A10}$$

(3) In this new representation calculate Eq. (A3):

$$\rho_{DQ}^{TT}(90) = (P^{TT})^{-1}\rho_{DQ}^{TT}P^{TT} = -a_x^{1-3}S_x^{2-3}. \tag{A11}$$

(4) The transformation of ρ_{DQ}^{TT} back to the rotating frame yields

$$\rho_{DQ}^{T}(90) = -(1/\sqrt{2})a_x^{1-3}(S_x^{2-3} - S_x^{1-2}) \tag{A12}$$

and

$$\rho_{DQ}^{90} = -\tfrac{1}{2}a_x^{1-3}(S_x^{2-3} + S_y^{2-3} - S_x^{1-2} - S_y^{1-2}). \tag{A13}$$

This result is used in Eq. (3.57).

The density matrix after the pulse will evolve, due to the quadrupolar interaction, as

$$\rho_{DQ}^{90}(t) = \exp[-\tfrac{2}{3}\omega_Q(S_z^{1-2} - S_z^{2-3})t]\rho_{DQ}^{90}\exp[\tfrac{2}{3}\omega_Q(S_z^{1-2} - S_z^{2-3})t]$$
$$= -(1/\sqrt{2})a_x^{1-3}[S_x^{1-2}\cos(\omega_Q t + \tfrac{1}{4}\pi) - S_y^{1-2}\sin(\omega_Q t + \tfrac{1}{4}\pi) + S_x^{2-3}\cos(\omega_Q t + \tfrac{1}{4}\pi) - S_y^{2-3}\sin(\omega_Q t + \tfrac{1}{4}\pi)]. \tag{A14}$$

The signal intensity corresponding to this density matrix equals

$$M_x(t) = \mathrm{Tr}[\rho_{DQ}^{90}(t)S_x] = \sqrt{2}\,\mathrm{Tr}[\rho_{DQ}^{90}(t)(S_x^{1-2} + S_x^{2-3})]$$
$$= -a_x^{1-3}\cos(\omega_Q t + \tfrac{1}{4}\pi) \tag{A15}$$

and the full double-quantum coherence a_x^{1-3} is transferred to the single-quantum signal intensity.

A 45° pulse at a phase angle of 90° with respect to the mixing pulse transfers only half of the double-quantum coherence to single-quantum coherence. In this case we must calculate

$$\rho_{DQ}^{45} = P^{-1}\rho_{DQ}P$$

with (A16)

$$P = \exp(-i\tfrac{1}{4}\pi S_x) = \exp[-i(\pi/2\sqrt{2})(S_x^{1-2} + S_x^{2-3})].$$

Transformation of ρ_{DQ}^{45} and P with U_y^{1-3} in Eq. (A8) results in

$$\rho_{DQ}^{T} = (U_y^{1-3})^{-1}\rho_{DQ}U_y^{1-3}$$
$$= a_x^{1-3}S_z^{1-3} = \tfrac{1}{2}a_x^{1-3}[S_z^{1-2} + (S_z^{1-3} + S_z^{2-3})] \tag{A17}$$

and

$$P^T = \exp(-i\tfrac{1}{2}\pi S_x^{1-2}).$$

With these equations we obtain

$$\rho_{DQ}^{T}(45) = (P^T)^{-1}\rho_{DQ}^{45}P^T$$
$$= \tfrac{1}{2}a_x^{1-3}S_y^{1-2} + \tfrac{1}{2}a_x^{1-3}(S_z^{1-3} + S_z^{2-3}) \tag{A18}$$

and transforming back

$$\rho_{DQ}^{45} = P^T\rho_{DQ}^{T}(45)(P^T)^{-1}$$
$$= (1/2\sqrt{2})a_x^{1-3}(S_y^{1-2} + S_y^{2-3})$$
$$+ \tfrac{1}{2}a_x^{1-3}(S_z^{1-3} + S_z^{2-3}). \tag{A19}$$

The signal intensity just after this pulse equals

$$M_y = \mathrm{Tr}(\rho_{DQ}^{45}S_y) = \sqrt{2}\,\mathrm{Tr}[\rho_{DQ}^{45}(S_y^{1-2} + S_y^{2-3})]$$
$$= \tfrac{1}{2}a_x^{1-3}. \tag{A20}$$

This result was used in Sec. V C to evaluate the signal intensities after a double-quantum cross-polarization experiment.

APPENDIX B

The rate equations for the spin temperature coefficients β_I and β_S can be written in matrix form[22]

$$\frac{d}{dt}\beta = -\Gamma\beta + \alpha, \tag{B1}$$

with

$$\beta=\begin{pmatrix}\beta_I\\ \beta_S\end{pmatrix},\quad \alpha=\beta_L\begin{pmatrix}R_{1D}\\ R_{1\rho}\end{pmatrix}, \tag{B2}$$

$$\Gamma=\begin{pmatrix}\epsilon R_{IS}+R_{1D} & -\epsilon R_{IS}\\ -R_{IS} & R_{IS}+R_{1\rho}\end{pmatrix} \tag{B3}$$

and in general $R_i=T_i^{-1}$.

To solve Eq. (B1) we diagonalize Γ and get

$$\Lambda=D^{-1}\Gamma D, \tag{B4}$$

with

$$\Lambda=\begin{pmatrix}\lambda_+ & 0\\ 0 & \lambda_-\end{pmatrix} \tag{B5}$$

and

$$D=\begin{pmatrix}\cos\theta & \epsilon\sin\theta\\ -\sin\theta & \cos\theta\end{pmatrix}, \tag{B6}$$

with the values for $\lambda_\pm$ and θ:

$$\lambda_\pm=\tfrac{1}{2}[(1+\epsilon)R_{IS}+R_{1\rho}+R_{1D}] \pm\tfrac{1}{2}\{[(\epsilon-1)R_{IS}+R_{1D}-R_{1\rho}]^2+4\epsilon^2R_{IS}^4\}^{1/2}, \tag{B7}$$

$$\sin2\theta=-R_{IS}\{[(\epsilon-1)R_{IS}+R_{1D}-R_{1\rho}]^2+4\epsilon^2R_{IS}^4\}^{-1/2}. \tag{B8}$$

The general solution of Eq. (B1) becomes

$$\beta=De^{-\Gamma t}D^{-1}\beta(0)+D(1-e^{-\Gamma t})D^{-1}D\Lambda^{-1}D^{-1}\alpha \tag{B9}$$

and with the initial condition

$$\beta(0)=\beta_L\begin{pmatrix}\omega_{0I}/\omega_I\\ 0\end{pmatrix},$$

we obtain

$$\beta_S(t)=\beta_Lg(t)=\beta_L\frac{1}{\cos^2\theta+\epsilon\sin^2\theta}\left(\sin\theta\cos\theta\frac{\omega_{0I}}{\omega_{1I}}(e^{-\lambda_-t}-e^{-\lambda_+t})+(\epsilon\sin^2\theta R_{1\rho}-\sin\theta\cos\theta R_{1D})\frac{1-e^{-\lambda_+t}}{\lambda_+}\right.$$
$$\left.+(\cos^2\theta R_{1\rho}+\sin\theta\cos\theta R_{1D})\frac{1-e^{-\lambda_-t}}{\lambda_-}\right). \tag{B10}$$

This expression was used in the computer program to fit the dynamics and the value of ϵ_D in the cross-polarization experiments.

*Based in part on the thesis of T. W. Shattuck, University of California, Berkeley, 1977, Lawrence Berkeley Laboratory Report No. LBL5458.

[1]S. Vega and A. Pines, J. Chem. Phys. 66, 5624 (1977).

[2]S. Vega, T. W. Shattuck, and A. Pines, Phys. Rev. Lett. 37, 43 (1976); G. Drobny, A. Pines, S. Sinton, D. Weidekamp, and D. Wemmer, Trans. Faraday Soc. (in press).

[3]A. Pines *et al.*, in *Magnetic Resonance in Condensed Matter-Recent Developments*, edited by R. Blinc and G. Lahajnar (Univ. of Ljubljana, Ljubljana, 1977), p. 128; S. Vega and A. Pines, in *Magnetic Resonance and Related Phenomena*, edited by H. Brunner, K. H. Hausser, and D. Schweitzer (Beltz Offsetdruck, Hemsbach, 1976), p. 395.

[4]H. Hatanaka, T. Terao, and T. Hashi, J. Phys. Soc. Jpn. 39, 835 (1978); H. Hatanaka and T. Hashi, *ibid.* 39, 1139 (1975).

[5]R. G. Brewer and E. L. Hahn, Phys. Rev. A 11, 1641 (1975).

[6]W. P. Aue, E. Bartholdi, and R. R. Ernst, J. Chem. Phys. 64, 2229 (1976).

[7]M. E. Stoll, A. J. Vega, and R. W. Vaugham, J. Chem. Phys. 67, 2029 (1977).

[8]M. E. Stoll, E. K. Wolff, and M. Mehring, Phys. Rev. A 17, 1561 (1978).

[9]D. E. Wemmer, Ph.D. thesis, University of California, Berkeley, 1979 (unpublished).

[10]U. Haeberlen and J. S. Wangh, Phys. Rev. 175, 453 (1977).

[11]S. R. Hartman and E. L. Hahn, Phys. Rev. 128, 2042 (1962); F. M. Lurie and C. P. Slichter, *ibid.* 133, A1108 (1964).

[12]P. Mansfield and P. K. Grannell, J. Phys. C 4, L197 (1971).

[13]A. Pines, M. G. Gibby, and J. S. Wangh, J. Chem. Phys. 59, 569 (1973).

[14]D. A. McArthur, E. L. Hahn, and R. Walstedt, Phys. Rev. 188, 609 (1969).

[15]D. E. Demco, J. Tegenfeldt, and J. S. Wangh, Phys. Rev. B 11, 4133 (1975).

[16]A. Abragam, *Principles of Nuclear Magnetism* (Oxford University Press, London, 1961).

[17]S. Vega, J. Chem. Phys. 68, 5518 (1978).

[18]A. Wokaun and R. R. Ernst, J. Chem. Phys. 67, 1752 (1977).

[19]A. Pines and T. W. Shattuck, Chem. Phys. Lett. 23, 614 (1973); T. W. Shattuck, Ph.D. thesis, University of California, Berkeley 1976 (unpublished).

[20]M. Kunitonio, J. Phys. Soc. Jpn. 30, 1059 (1971).

[21]R. R. Ernst, in Proceedings of the 4th EENC, Grenoble, France, 1979 (unpublished).

[22]H. Levanon and S. Vega, J. Chem. Phys. 61, 2267 (1974).